8-2017

Chaperoning EF Hands that Shape Calcium Response: NCALD, HPCA and S100B

Jingyi Zhang
Rowan University

CHAPERONING EF HANDS THAT SHAPE CALCIUM RESPONSE: NCALD, HPCA AND S100B

Jingyi Zhang, B.S.

A Dissertation submitted to the Graduate School of Biomedical Sciences, Rowan University in partial fulfillment of the requirements for the Ph.D. Degree.

Stratford, New Jersey 08084

August 2017

Table of Contents

Acknowledgements

It has been an amazing and challenging journey since 2010, when I joined the GSBS program. I would like to thank Dr. Hock, Dr. Worrad and the rest of GSBS staff for their help in completing my thesis work and helping me as an international student, through the journey. I am also grateful to Dr. Waterhouse, the Chairman of Cell Biology and Neuroscience department.

Nobody deserves more acknowledgement than my mentor, Dr. Venkataraman, for his patient guidance in experimental design and data interpretation. I have learnt a lot from him, about science, techniques and also how to be a good person in life. I also want to thank Dr. Krishnan for her guidance on science and her contribution to my growth. Many thanks to both of them for being family to me for many years.

I sincerely thank my committee members Dr. Gary Goldberg, Dr. Robert Nagele, Dr. Joseph Martin and Dr. Bradford Fischer for their support and criticism on my work.

I would like to thank my lab mates, Dr. Hao Wu, Dr. Jeff Viviano for over 6 years of company. Both of them are very intelligent and considerate and I really enjoyed working with them. Thanks for their emotional as well as scientific support. I also want to thank Pooja Amin for her contribution on my thesis work.

I also would like to thank my parents and my husband for their great support and understanding.

Abstract

All organisms have an internal clock with a defined period between repetitions of activities. The period for circadian clock in human is 24.5 hours, while in mouse and rat, it is 23.5 hours. However, all organisms are forced to be in synchronization with their environment. A major environmental force that resets the internal clock to 24 hours is light. This phenomenon is defined as "light entrainment" or "phase-setting". It is unclear how this entrainment process occurs. Studies from this laboratory indicate a role for two neuronal calcium sensor proteins: Neurocalcin δ (NCALD) and S100B. For these two genes, mRNA as well as protein levels exhibit a light-dependent variation, which is observed both in a cell line (derived from SCN progenitors) as well as selected tissues in rats and mice. We hypothesize that the two proteins interact with each other and their ability to translocate upon a spike in intracellular calcium is critical for their function. Here, we demonstrate that NCALD and S100B interact with each other both *in vivo* and *in vitro*. The interaction is likely modulated by free calcium concentrations under both conditions. We also demonstrate that the NCALD-S100B complex translocates to a peri-nuclear, vesicle-rich location upon histamine addition in COS7 cell line, whereas the S100B-S100B complex does not. The results suggest that NCALD serves as a calcium-dependent chaperone for S100B, enabling targeting of the complex to certain intracellular locations to accomplish different tasks.

1. Introduction

All organisms are forced to be in synchrony with their environment. The onset of light and darkness (due to earth's rotation around the sun) forces a 24-hour lifestyle with alternating periods of activity and inactivity. All vertebrates are endowed with an innate body clock that runs to around 24 hours. This clock is defined as the circadian clock. The central clock in the body is located in the Suprachiasmatic Nucleus (SCN), a collection of about 20,000 neurons located close to the chiasm of the two optic nerves on either side of the third ventricle in the hypothalamus. The period for this clock in human is 24.5 hours, while in mouse and rat, it is 23.5 hours. However, under normal environmental conditions, the period (in human, mouse and rat) is set to 24 hours by light. This phenomenon is defined as "light entrainment" or "phase-setting" [reviewed in: [1, 2]]. Irregularities in this physiological process lead to serious diseases such as narcolepsy (observed in night-shift workers) and inconveniences such as jet lag [reviewed in: [3]]. However, to this day, the exact mechanism by which light entrains the circadian clock remains to be elucidated.

Some key molecules involved in the entrainment process have been identified through work from our and other laboratories. Based on current research, the understanding is that light is detected by non-visual photoreceptors in the retina and the information is conveyed to a sub-population of SCN neurons by the retino-hypothalamic tract (RHT) via release of glutamate. It results in an elevation of intracellular calcium and cyclic GMP, activating downstream pathways that

eventually result in phase-setting [reviewed in: [4]]. However, the link between calcium and cyclic GMP and the identities of the protein molecules involved remains unknown.

Circadian Rhythm:

The circadian center in mammals is localized in the suprachiasmatic nucleus (SCN) located close to the chiasm of the two optic nerves. It receives signal from retina and multiple auxiliary brain regions and regulates downstream oscillators in peripheral tissues. As the base of circadian rhythm, the molecular oscillators are based on transcriptional and post-translational feedback loops [reviewed in: [5]] These molecular oscillators are thought to drive circadian rhythmicity in pacemaker cells and provide an endogenous period which is not exactly 24 h. However, the period is adjusted to match the external photoperiod to 24 h, by light, which is called light entrainment [reviewed in: [1, 2]].

Calcium and Cyclic GMP in light entrainment:

An important second messenger in circadian photic entrainment is calcium, which is the key component of the molecular pathways linking the oscillation of clock genes expression and output [reviewed in: [4 , 6-8]]. Calcium is mobilized through membrane channels and intracellular reservoirs, which leads to an increase in intracellular levels and activation of many enzymes and pathways. It has been demonstrated that light activates cGMP-dependent protein kinase and that this step is critical for photoentrainment, which suggests that cGMP is involved in light entrainment [reviewed in: [7, 8]]. However, the mechanism by which calcium and cGMP are linked in light entrainment remains to be elucidated.

Link between calcium and cyclic GMP:

The link between calcium and cyclic GMP has been clarified predominantly by researchers in the field of phototransduction, where light, calcium and cyclic GMP are interlocked in a negative feedback regulatory loop. Light causes reduction in cyclic GMP levels through activation of phosphodiesterase, leading to closure of cyclic nucleotide-gated calcium channels. This results in hyperpolarization. Restoration to ground state occurs by up-regulation of membrane guanylate cyclase (mGC) by calcium-sensor proteins GCAP1 and GCAP2. Subsequently, the interplay between calcium and cyclic GMP through mGC and calcium-sensor proteins have been demonstrated in multiple neuronal systems [[9-11]; reviewed in: [12-15]]. These studies have highlighted the role for the group of calcium sensor proteins, which are now classified under the neuronal calcium sensor (NCS) protein superfamily. NCS proteins play a crucial role in mediating Ca^{2+} signaling. They are expressed in neurons and bind to calcium through EF hand motifs. Most NCS proteins can become membrane-associated by using a N-terminal myristoylation group [reviewed in: [16]]. Numerous NCS proteins have been identified in vertebrate, including S-modulin, visinin, visinin-like proteins (VILIPs), frequenin, hippocalcin, and multiple isoforms of neurocalcins. [17]. This thesis, focuses on three NCS proteins: neurocalcin delta (NCALD), closely-related hippocalcin (HPCA) and S100B.

Why NCALD?

NCALD is primarily expressed in the central nervous system, spinal cord, retina, inner ear, olfactory epithelium and zona glomerulosa of the adrenal gland [17, 18]. It consists of four EF hands although EF1 hand is disabled from binding calcium. A major feature of NCALD is N-terminal myristoylation, which allows NCALD to interact with cell membrane. The myristoyl group is sequestered within the protein in the Ca^{2+} free state. When the protein binds to Ca^{2+}, the myristoyl group extrudes, allowing it to interact with membrane [18, 19]. Upon the elevation of intracellular Ca^{2+}, NCALD is translocated to the perinuclear compartment from cytosol [20]. A critical role of NCALD in photic entrainment is predicted based on the following studies/facts: (i) it is known to stimulate mGC in a calcium-dependent fashion [10] (ii) NCALD expression has been localized to subset of SCN neurons that interface with the RHT [21]; (iii) Additionally, NCALD is expressed in the retina in many species in a subpopulation of ganglion cells that may be the non-visual photoreceptors critical for entrainment [22] , and; (iv) finally, previous data from our laboratory show that NCALD exhibits a light-dependent variation in both mRNA and protein levels in two systems: an immortalized SCN cell line as well as rat or mouse organ systems.

Why S100B?

The S100 proteins are a group of proteins which consist of at least 25 members in human, including S100B. The proteins are dimeric having two “EF-hand” calcium binding motifs in each subunit. Most S100 proteins can bind calcium

and undergo a conformational change which allows them to control cellular activity by interacting with other proteins [reviewed in:[23]]. S100B is one of the target proteins of NCALD suggesting that the S100B-NCALD complex may be involved in Ca^{2+} signaling in the glial cell [24].

Why HPCA?

Hippocalcin is a protein closely related to NCALD, and shares an 88% identity and 95% similarity with NCALD. Both proteins have 193 residues, a myristoylated N-terminus, and 4 EF hands in which the first hand is not functional. However, data from our lab showed that the calcium sensitivities of these two proteins are very different. HPCA was originally purified from the hippocampus [25] and has been demonstrated to be critical for long term potentiation of memory (LTP). Mice that lack HPCA function have demonstrated impaired long-term memory [26] and creating spatial memories [27]. The phenotype of losing LTP in HPCA knockouts, which showed no change of expression in other NCS proteins, demonstrates that NCALD cannot compensate for HPCA [26].

Recently, mutations in the HPCA gene have been identified to be critical in autosomal recessive primary-isolated dystonia [28]. The molecular mechanisms of how HPCA functions remain to be elucidated. Its structural relation to NCALD has made the protein a focus of our laboratory, especially in dissecting any functional differences between HPCA and NCALD.

Significance

It is a well-documented fact that circadian rhythms are critical for normal physiological processes (sleep, heartbeats, hormonal changes) [2, 29] as well as disease states (cancer, mood disorders, metabolic disorders, seasonal affective disorder) [30-33]. The disturbance of circadian rhythm is also an early sign for some diseases, such as acute renal failure [34]. In addition, it has been shown that cancer is closely related to circadian rhythm [35]. These rhythms also regulate key clinical indicators (blood pressure, serum cortisol) and are recognized as critical in diagnosing and treating patients [36, 37]. Coordination of the timing of administration of medicine for treatment with the circadian clock is critical for the efficiency of the treatment and avoidance of drug toxicity [38]. Studies show that changes in circadian rhythm can affect stress and productivity for some animals [39].

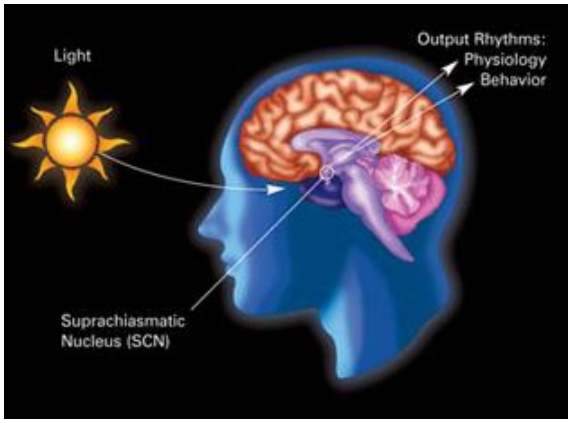

Figure 1.1: SCN and entrainment
http://www.nigms.nih.gov/Education/Pages/Factsheet_CircadianRhythms.aspx

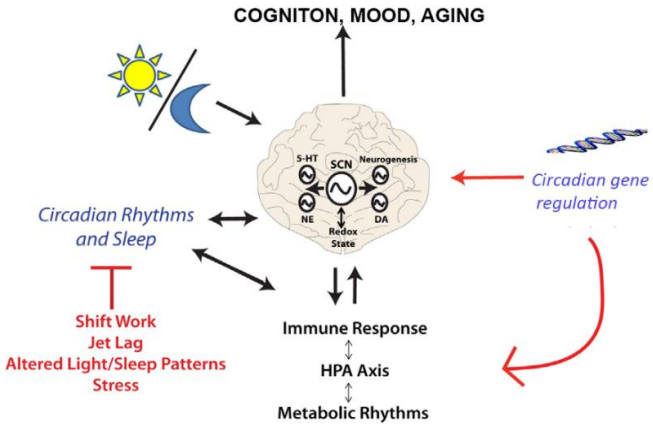

Figure 1.2: Clock regulation and impact
Adapted from McClung, Biol Psychiat, 2013

The molecular clock is a biological network of fundamental value in the

harmonization of human biology with the external environment and influences the diurnal variability of our activity, body temperature, mood, blood pressure, and patterns of hormonal secretion [40]. The endogenous "master clock" – SCN- entrains to changing light cycles, aligning our behavior with seasonal changes in day length or, for the world traveler or shift worker, light presentation (Fig. 1.1). However, systemic signals, entrained by the SCN, particularly temperature, may also impinge on peripheral clocks. Such influence results in a widespread effect on multiple physiological processes (Fig. 1.2).

Research over several decades has identified an underlying Transcription-Translation-Feedback-Loop (TTFL) that regulates the clock [41]. Several key genes have also been identified. ***However, a major gap exists in our understanding of how light regulates and entrains the endogenous SCN-driven clock***. This thesis was originally designed to investigate the possibility that the calcium sensor proteins, NCALD and S100B may play a critical role in this process. The results obtained, however, indicate a more fundamental role for NCALD, HPCA and S100B in determining cellular (neuronal) responses to calcium.

2. Rationale

Studies from this laboratory indicate a role for two neuronal calcium sensor proteins - Neurocalcin delta (NCALD) and S100B – in photoentrainment. For these two genes, mRNA as well as protein levels exhibit a light-dependent variation, which is observed both in a cell line (derived from SCN progenitors) as well as in rats and mice.

Hypothesis: NCALD and S100B interact specifically with each other and their ability to translocate to specific locations in the cell upon a spike in intracellular calcium is critical for their function in photoentrainment. The following questions guided the experimental design:

1. Is there evidence that NCALD and/or S100B may be involved in circadian rhythms?
2. Do the two proteins interact with each other with high specificity?
3. At the cellular level, what is the response of NCALD and S100B to changes in calcium?
4. Are there other external signals that these proteins may also respond to?

Some of these questions are answered in specific chapters. The results also argue that NCALD and HPCA, together with S100B, may shape cellular responses to calcium through their interaction. In addition, they may also serve as redox sensors. Some of these findings are also discussed.

3. Materials and Methods

Plasmid construction:

Generation of fluorescent protein-tagged constructs for mammalian expression:

Rat hippocalcin (HPCA) and neurocalcin δ (NCALD) coding regions were amplified and inserted in frame between HindIII and BamH1 sites of the expression vector pcDNA3-EYFP (Addgene). The primers for HPCA were: sense primer with a HindIII site (5'-ACG TAA GCT TAT GGG CAA GCA GAA TAG CAA GCT GCG G-3') and antisense primer with a mutated stop codon containing the BamH1 site (5'-CAT TGG ATC CCG GAA CTG GGA AGC GCT GCT GGG-3') to enable continuous reading in-frame into the fluorescent protein coding sequence. The primers for NCALD were: sense primer with a HindIII site (5'-ACG TAA GCT TAT GGG GAA ACA GAA CAG CAA GCT GCG C -3') and antisense primer with a mutated stop codon containing the BamH1 site (5'-CAT TGG ATC CCG GAA CTG GCC GGC ACT GCT GGG -3').

To generate chimeric constructs of NCALD and HPCA (NCHC and HCNC), the coding region from the previously generated construct for bacterial expression [42] was amplified and inserted in place of wild-type protein. Point mutations were created using the QuikChange II XL Site-Directed Mutagenesis kit from Agilent Technologies. All constructs were confirmed via sequencing. Generation of the W30F and W103F mutants of NCALD for bacterial expression have been described earlier [43] and were used to construct the plasmid for mammalian expression. To create the T71N and N75K mutants of HPCA linked to dystonia, the following primer pairs were used: T71N – 5'CAT GTC TTC CGC AAT TTT GAC ACC AAC -3' and 5'-

GTT GGT GTC AAA ATT GCG GAA GAC ATG -3'. N75K - 5'- ACT TTT GAC ACC AAA GCG ACG GCA CCA -3' and 5'- TGG TGC CGT CGC TTT GGT GTC AAA AGT -3'.

COS-7 cell culture and transfection

The COS-7 cells were cultured in DMEM (Dulbecco's Modification of Eagle's Medium) medium with 1g/L glucose, L-glutamine and sodium pyruvate (CORNING) supplemented with 10% fetal bovine serum (Hyclone), at 37 °C in an atmosphere containing 5% CO_2.

COS7 cells were transfected, using calcium phosphate buffer with either an expression plasmid for hippocalcin (pcDNA3-Hippocacin-EYFP) or the control vector (pcDNA3-EYFP) without HPCA, using standard protocols [44]. Briefly, the transfection mixture containing HEBS buffer [25 mM HEPES, 140 mM NaCl and 0.75 mM Na_2HPO_4, (pH 7.05)], 250 mM $CaCl_2$, and 15 μg of plasmid DNA was incubated at room temperature for 30 min and added to COS-7 cells in 35mm dishes. After further incubation at room temperature for 30 min, fresh medium was added. Cells were grown for 24 h, and the expression of the fluorescent tagged proteins was analyzed using a C2 confocal laser scanning microscope (Nikon) equipped with Tokai-Hit stage for live imaging. Images were obtained following Hoechst addition (2 μg/ml) before and after histamine addition (45 μM).

The images were processed in Fiji (ImageJ). Vibrations of the microscopy, mechanical relaxation and thermal fluctuation often cause sample drift in the images especially during a time course experiment. In order to compensate for this, an image stabilizer plug-in for ImageJ (http://www.cs.cmu.edu / ~kangli/code/

Image_Stabilizer.html) was used for each field. A correction based on the Lucas-Kanade algorithm was calculated using the DIC image. The same correction was then applied to all channels of the image stack (for instance, the DIC, the green channel for detecting the YFP signal and the blue channel to view the nucleus). The fluorescent intensity was measured. The statistical analyses for comparing the mean differences between the methods, performing regression analyses for each method, and plotting the comparison curves were performed with either Prism or SPSS 24. Two-tailed tests of statistical significance were set for all analyses and are indicated by *P<0.05, ** P<0.01, *** P<0.001.

Protein expression and purification:

pET 21d plasmids encoding NCALD, HPCA, NCHC, HCNC and all the mutants were transformed into *E. coli* ER2566 cells which co-expressed yeast N-Myristoyl Transferase. The cells were induced with IPTG. Myristic acid was added to the cells to generate myristoylated form of the proteins, which were then purified by calcium dependent Hydrophobic Interaction Chromatography using phenyl sepharose as described previously [18]. After concentration, the proteins were washed with calcium-depleted 20 mM Tris HCl (pH 7.5) to remove the bound calcium. At least three preparations of 2 different clones were purified and tested.

Western blot

Detection of NCALD and S100B in SCN2.2 cells via western blotting was carried out according to protocols routinely used in the laboratory [9, 45-47]. It is briefly described below: 50 μg of protein per lane was loaded onto the SDS-12% poly acrylamide gel alongside PageRuler™ Prestained Protein Ladder Plus (Life

Technologies, Cat# 26616). Proteins were separated at 135 V for 75 min and then transferred to Hybond-ECL Nitrocellulose Membrane (GE) on ice using Bio-Rad Mini Protean II apparatus. Blocking of non-specific binding was accomplished by incubation in 5.0% non-fat milk in PBS-Tween (PBS-T, 0.05% Tween20) buffer. The blot was incubated with the primary antibody diluted in the same buffer, overnight at 4°C. After washes with PBS-T, the blot was incubated with peroxidase-conjugated secondary antibody (diluted at 1: 20,000) for 1 hour at 4°C, washed, developed using SuperSignal West Femto Maximum Sensitivity Substrate (Thermo Scientific/Pierce, IL, USA) and then auto radiographed.

Membrane overlay

Two μg of NCALD, HPCA or a derivative were spotted onto nitrocellulose and blocked with 3% BSA in TBS-T for 1 hr at room temperature. The membrane was then incubated with 80 nM of S100B in 50mM Tris HCl, pH 7.4, 0.1% Tween-20, 150mM NaCl, 1mM $MgSO_4$,1mM DTT, in the presence of indicated concentrations of $CaCl_2$ (0, 0.5mM and 1mM). After 1h incubation, the blot was washed with the same buffer. Bound S100B was detected using monoclonal antibody (Sigma-Aldrich) following standard western blotting protocol and ECL detection. Quantification was through ImageJ.

Bimolecular fluorescence complementation

Sequences encoding NCALD and S100B were fused to sequences encoding the N- (residues 1-158) and C- terminal EYFP (residues 159-238) fragments respectively in expressing vector pcDNA1 (A kind gift from Dr. Berlot, Weis Center for Research, Danville, PA).

Constructs were transfected into COS-7 cells using calcium phosphate buffer. Experiments were carried out after 48 h post transfection. Images were acquired using a Nikon C1 laser confocal microscope equipped with a TokaiHit on-stage incubator. All images were captured using identical parameters such as exposure time, pinhole size etc. NIH ImageJ [48] was used to quantify the images. Positive cell numbers were calculated and plotted in Prism.

Direct calcium binding assay

^{45}Ca overlay was carried out according to Maruyama et al (1984). Briefly, purified proteins were separated on an SDS-12% polyacrylamide gels and then transferred to nitrocellulose. The blot was washed in imidazole buffer (10 mM imidazole HCl, 60 mM KCl, 5 mM $MgCl_2$, pH 6.8) for 45 min with buffer changes every 15 min. The washed blot was incubated in 2 μCi of $^{45}CaCl_2$ per ml of imidazole buffer for 30 min at room temperature. The blot was then washed for 2 min with distilled water and then for 30sec with 50% ethanol, air-dried and imaged using a phosphor imager. The band intensity was measured using ImageJ and plotted using Prism.

Guanylate cyclase activity assay:

The Guanylate cyclase activity assay was carried out as described previously [49, 50]. Membranes of COS cells transfected with ROS-GC1 served as the source of the enzyme for guanylate cyclase activity assay. Briefly, membranes were pre-incubated on ice with or without NCS protein in a reaction mix containing 10 mM theophylline, 15 mM phosphocreatine, 20 μg creatine kinase, 50 mM Tris–HCl, pH 7.5. Incubation was carried out in the presence or absence of calcium (10 μM). The

total assay volume was 25 µl. The reaction was initiated by the addition of the substrate solution (to a final concentration of 4 mM $MgCl_2$ and 1 mM GTP), followed by incubation at 37°C for 10 min. The reaction was terminated by the addition of 225 µl of 50 mM sodium acetate buffer, pH 6.2 and heating on a boiling water bath for 3 min. The mixture was spun down at 3000 rpm for 10 mins and the supernatant was used to measure the amount of cyclic GMP formed using DetectX direct cGMP immunoassay kit according to manufacturer's protocol (Arbor Assays).

Tryptophan fluorescence

Fluorescence measurements were carried out on a Fluromax -3 spectrofluorimeter. Tryptophan emission fluorescence spectra were recorded at 22°C from 0.1 ml samples with 4 µM HPCA in 20mM Tris pH 7.5. The excitation wavelength was set at 290 nm (bandwidth, 4 nm), and the emission wavelength was varied from 300 to 400 nm (bandwidth, 4nm). Samples were incubated with buffer containing increasing concentrations of calcium using calcium calibration buffers purchased from Molecular Probes by Life Technologies.

Growth and synchronization of SCN cells:

SCN 2.2 cultures were maintained in growth medium (GM) according to standard protocols (Allen and Earnest, 2002; Earnest *et al.*, 1999a; Hurst *et al.*, 2002a). For synchronization experiments, they were grown to confluence on laminin-coated plates in GM. After 24–48 h at 100% confluence, serum-free neuronal medium (NM) was added instead of the growth medium to promote differentiation. After 72 h in NM, SCN 2.2 cultures were serum-shocked for 2h with 50% FBS in NM followed by a rinse with 50% DMEM/50% Ham's F12 media. Control cultures were treated the

same in every way except that NM was used without FBS. Cultures were immediately returned to NM, harvested at different time intervals for 24 h. Collection time points began immediately after serum-shock (0 h). Due to the possibility of a phase-dependent response of SCN2.2 cells to differing treatment, all cultures (within the same experiment) were split and exposed to media changes and serum-shock in parallel [51].

Isolation of SCN membranes:

Cultured SCN cells were washed twice with 50 mM Tris-HCl (pH 7.5)/10 mM $MgCl_2$ buffer, scraped into 2 ml of cold buffer, homogenized, centrifuged for 15 min at 5000*g* and washed several times with the same buffer. The resulting pellet represented the membrane fraction. For the tissue, dissected SCN region was obtained and homogenized in the above buffer containing 0.25M sucrose, followed by differential centrifugation to obtain the membrane fraction [9, 47, 52].

RT-PCR analyses:

RNA isolation was carried out according to the manufacturer's protocols (Roche Pharmaceuticals). DNA-free RNA was then converted into cDNA with reverse transcriptase (Clontech) and specific fragments were amplified. The reaction mixture was electrophoresed on 1% agarose gel and the product purified and sequenced using internal primers. Water instead of RNA or RNA with only one primer was used as a negative control (***Control***) – no product was observed in either case.

For semi-quantitative RT-PCR, RNA was isolated from SCN 2.2 cells synchronized as described above at indicated time points. Equal amounts of DNA-

free RNA were converted into cDNA and fragments encoding NCALD, S100B and L30 were amplified. The PCR products were electrophoresed on an agarose gel and the intensity of the amplified product was quantified. For Real Time PCR, the RNA was converted into the cDNA using the manufacturer's protocol (Clontech). Real time PCR reactions were carried out on an ABI 7500 system using the SYBRgreen protocol. Efficiency testing was performed for all primer pairs, based on linear regression analyses of C_T values plotted against the amount of template used. Efficiencies were comparable for all primer sets. Dissociation curves were performed following every reaction to ensure the fidelity of the reaction. All PCR products obtained have been sequenced (Genewiz) for confirmation. These analyses were performed for NCALD, Per1 and Clock. Amplification of L30 (encoding a protein of the large ribosomal subunit) was used for normalization, since it is endogenously expressed and its levels are not dictated by endogenous rhythms. Samples were run in triplicate and their C_T values were averaged. Data was analyzed using SDS v2.2.2, and the $\Delta\Delta C_T$ method was used to calculate relative quantitation with the samples normalized to the 0h time point.

Native Gel Electrophoresis (CIMSA):

Purified proteins were separated by native discontinuous (12%) PAGE (pH 8.8) at a constant voltage of 165 V for 2.5 hr in running buffer comprised of 25 mM Tris base and 190 mM glycine as previously described. Five μg of each of the proteins (at 1μg/μl) was mixed with 15μl of buffer containing specific concentrations of the free calcium using the calcium calibration buffers. Increasing calcium concentrations were obtained by mixing 0 μM and 39 μM calibration buffers from

Molecular Probes by Life Technologies. 5 μl of 6x Sample buffer (Laemmli sample buffer without SDS) was present in all samples [53, 54]. After electrophoresis, proteins were visualized with Coomassie blue R250. The relative mobility value for each band was measured using ImageJ. The data presented is compiled from several replicates analyzed and presented as mean ± SE using Prism 6.0. Statistical significance between indicated groups was determined by two-tailed student's *t* tests.

Statistics

Statistical significance was determined by a two-tailed Student's *t* test. *, $P<0.05$; **, $P<0.01$; ***, $P<0.001$. Mean ± SEM was used to represent the variations within each group.

4. Experimental Results

4.1: Neurocalcin δ - a role in light entrainment of the biological clock?

ABSTRACT

Cyclic GMP plays a critical role in setting the phase in circadian rhythms. However, the mechanism by which it is regulated is unclear. The results from this study suggest that membrane guanylate cyclase is the source and that its activity is regulated by the neuronal calcium sensor protein neurocalcin δ. This would also enable a tight coupling of the system to calcium, which is already an established regulator of the generation and maintenance of circadian rhythms.

INTRODUCTION

The SCN is the primary pacemaker in mammals, responsible for the co-ordination of the wakefulness and sleep to the environmental light-dark cycle ([55, 56]; reviewed in: [57]). Perception of the light dark cycles in the retina is communicated to the SCN via the RHT. Ca^{2+} oscillations have been suggested to play a role in both generating endogenous rhythms and photic entrainment [58]. Studies in mice lacking calbindin, a Ca^{2+} sensor protein, [59] and in *D. melanogaster* by buffering intracellular Ca^{2+} through the Ca^{2+}-binding protein parvalbumin [60] demonstrate importance of calcium. Circadian Ca^{2+} oscillations have been demonstrated in both plant and animal cells [61, 62]. Ca^{2+} influx also mediates the phase-setting action by light or neurotransmitters in SCN [63, 64].

Another molecule involved in phase setting is cyclic GMP (cGMP). It exhibits a diurnal rhythm in the SCN neurons, with its levels being maximal during the subjective day [65, 66]. Administration of cGMP induces phase advances when applied during the subjective night in rat hypothalamic slices [67] and inhibitors of cGMP synthesis prevent phase shifts [68]. Thus, phase setting in SCN requires the activation of a guanylate cyclase (GC). A role for the nitric oxide (NO)-regulated GC has been suggested (reviewed in: [69]); however, loss of NO synthase in mice has no effect on circadian rhythms [70, 71]. It has been suggested that phosphodiesterase may help regulate cGMP and cGMP-dependent protein kinase activity levels [69]. To date, no report is available on the presence of mGC in SCN that synthesizes cGMP independent of NO.

There are seven known mGCs [72] which comprise two subfamilies: surface receptor and calcium-regulated mGC (CaRGC). Members of the surface receptor subfamily are activated by peptide hormones or bacterial toxins. There are three members of this subfamily: ANFRGC, CNPRGC and STaRGC (also referred to as GC-A, GC-B, and GC-C, respectively) that are receptors, respectively for ANF [73, 74], CNP [75], stable bacterial enterotoxin (STa) and an intestinal peptide, guanylin [76, 77] [reviewed in: [72, 78, 79]]. These cyclases are activated by extracellular ligands. In contrast, members of the CaRGC subfamily respond to intracellular Ca^{2+} signals. There are three CaRGCs: ROSGC1 (or retGC1, GC-E), ROSGC2 (or retGC2, GC-F) and ONEGC (or GC-D) [reviewed in: [80, 81]]. CaRGC forms have been identified in the olfactory neurons [10, 52], retinal neurons [45, 82-85], hippocampus [50] and the pineal gland [9, 47]. In these cells, five major calcium-

dependent regulators have been demonstrated to modulate its activity: GCAP1, GCAP2, NCALD, S100B and HPCA. A model was proposed for the linkage between mGC and calcium in neurons [15, 81]. However, to date no information is available if the system is expressed in the SCN or whether it may be involved in circadian rhythms.

This study, for the first time, demonstrates the existence of the mGC transduction system in the SCN, identifies the SCN components of the system and presents results suggesting that the system contributes to the generation and/or maintenance of circadian rhythms in response to light.

MATERIALS AND METHODS

Described in Section 3

RESULTS & DISCUSSION:

SCN membranes contain a membrane guanylate cyclase: it is calcium-sensitive and exhibits oscillations

In order to determine if there was an mGC present in the SCN, membrane fraction from the SCN 2.2 cell line or dissected SCN tissue was isolated and examined.

In both cases, mGC activity was detected and comparable: ~ 0.2 pmol cGMP/min/mg protein. To test if the mGC was Ca^{2+}-sensitive, membranes were incubated in the presence of 1mM EGTA (-Ca^{2+}) or 100 μM calcium (+ Ca^{2+}). The results shown in figure 4.1.1A demonstrate that addition of calcium to the assay

results in an increase in mGC activity to 0.6 pmol cGMP/min/mg protein, ~ 3-fold (Fig. 4.1.1A: SCN).

Thus, there is, indeed, a Ca2+-modulated mGC present in this tissue. Similar results were obtained with membrane preparations from the SCN 2.2 cell line, which is derived from SCN progenitor cells (Fig. 4.1.1A: SCN cells). It is noted that similar changes have been observed in the olfactory neurons and retinal synaptic layers where the presence of a CaRGC has been demonstrated [10, 45, 52].

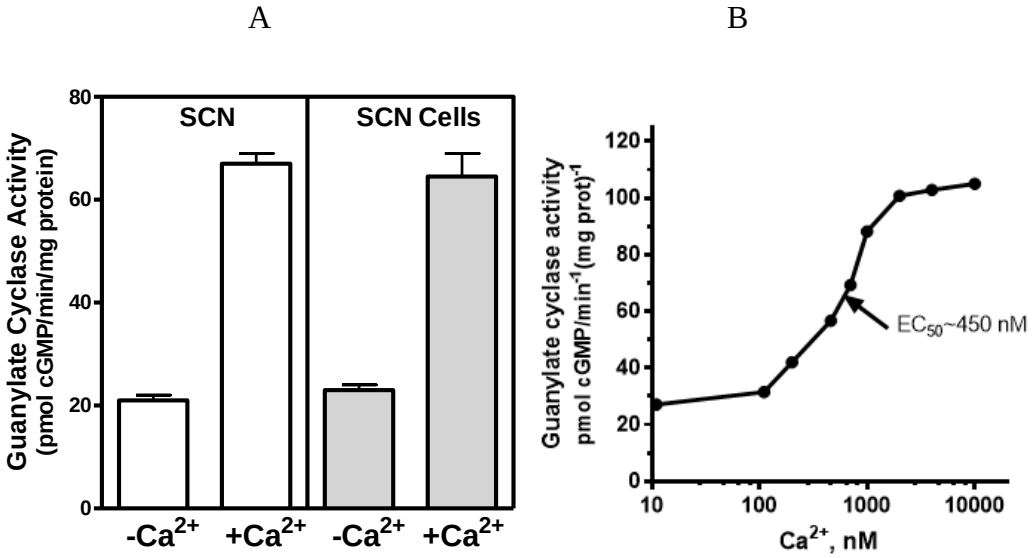

Figure 4.1.1: Presence of a calcium-dependent MGC in the SCN:

A. Membrane fractions were isolated from the SCN 2.2 cell line or dissected SCN tissue from rat. Guanylate cyclase activity was assayed for in the absence (-Ca^{2+}; contains 1 mM EDTA in assay) or presence of Ca2+ (+Ca^{2+}; contains 500 nM $CaCl_2$ in assay).

B. Membrane fraction was isolated from rat SCN 2.2 cells. Guanylate cyclase activity was assayed in the presence of incremental calcium concentrations. Experiments were carried out in triplicate.

Is the response to calcium dose dependent?

In order to investigate if the response was dependent upon the dose of calcium, the experiments were repeated with incremental concentrations of calcium in the assay mix. The results presented in figure 4.1.1B show that the SCN membrane guanylate cyclase activity is activated in a dose-dependent fashion by calcium with an EC_{50} of ~450 nM. Thus, the SCN membranes house a guanylate cyclase that is activated in the presence of incremental calcium.

Identity of mGC

As a first step towards determining the identity of the mGC, the mGCs expressed in the SCN were surveyed by RT-PCR. Specific primers were synthesized to enable amplification of each known mGC and used for analyses with RNA from cell line as well as SCN tissue. The results are presented in figure 4.1.2A. Only two known mGCs – ANFRGC and CNPRGC -- were detected. It is noted that none of the established mGCs known to be regulated by calcium – ROSGC1, ROSGC2 or ONEGC – were detected by RT-PCR.

Functional confirmation

In order to functionally determine the presence of ANFRGC and CNPRGC in the SCN, membranes were isolated and tested for response to ANF and CNP – the corresponding regulators of the mGCs. Addition of ANF or CNP resulted in a 2.5- to 3-fold increase in mGC activity in both SCN tissue and the cell line (Fig. 4.1.2B). The increase was also dependent on the dose, with a higher response at 10^{-6} M in both cases. Thus, the molecular evidence for the presence of the two cyclases is confirmed

by functional analyses. Interestingly, neither mGC is known to be regulated by calcium to date.

Identity of the SCN MGCs – Molecular and Biochemical Evidence:

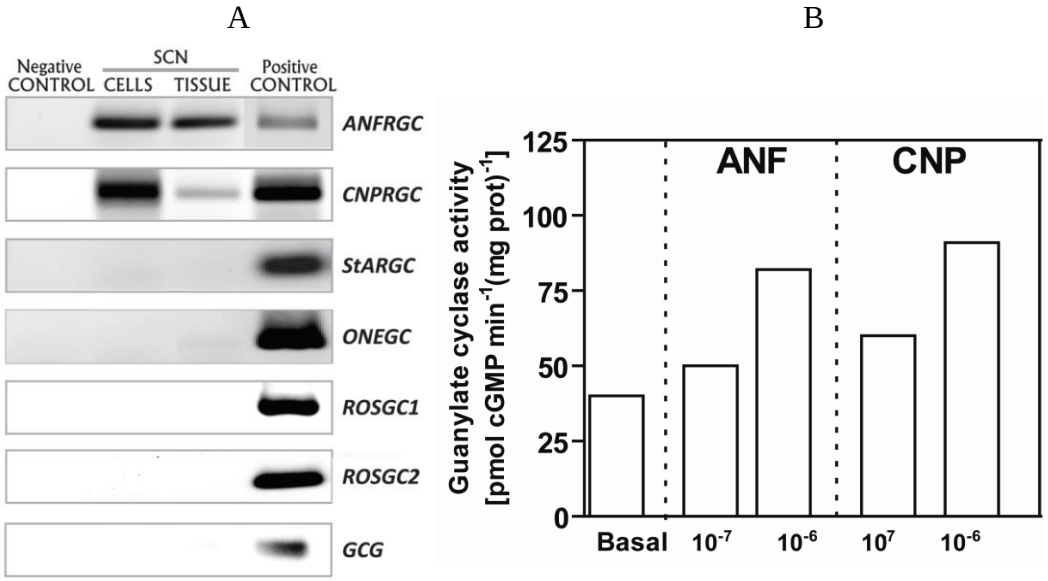

Figure 4.1.2: SCN has more than one mGC- Molecular and Biochemical evidence:

A. RNA was isolated from dissected rat SCN tissue, SCN cell line, eye and small intestine. Specific primers were directed against all known mGCs and were used to amplify the corresponding regions from SCN cDNA. Identical reactions without any template or with only one primer served as negative control. Positive controls were: ANFRGC, CNPRGC, ROSGC1, ROSGC2 – eye, ONEGC – plasmid, STaRGC and GCG – Small intestine. All PCR products obtained were sequenced to confirm their identity.

B. Membrane fraction was isolated from rat SCN and assayed for guanylate cyclase activity in the presence or absence of known mGC regulators. Data is presented for ANF, CNP and Guanylin, which were added at the indicated concentrations. All experiments were repeated at least thrice.

Identification of the regulator

In order to gain further insight into the CaRGC regulation in SCN, in the absence of a known CaRGC, experiments were designed to investigate the presence

of NCS proteins known to regulate the cyclases. The results obtained are presented in figure 4.1.3.

A B

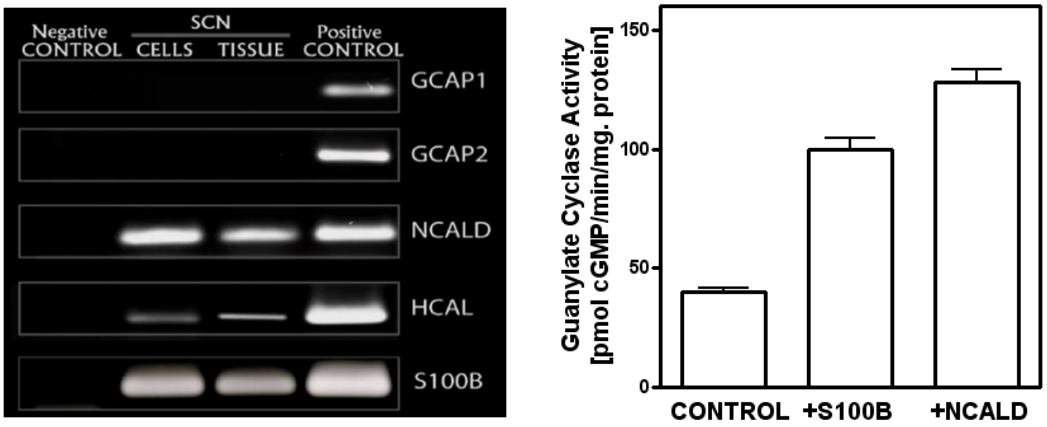

Figure 4.1.3: SCN expresses Ca^{2+}-dependent activators of mGC- Molecular and Biochemical evidence:

A. RNA was isolated from dissected rat SCN tissue, a SCN cell line, and eye. Specific primers were directed against known calcium-dependent regulators of MGCs and were used to amplify the corresponding regions. Identical reactions without any template served as a negative control. Positive controls were: GCAP1, GCAP2, S100B – eye; NCALD, HCAL – plasmid. All PCR products obtained were sequenced to confirm their identity.

B. Membrane fraction was isolated from rat SCN and assayed for guanylate cyclase activity in the presence or absence of S100B or neurocalcin δ. The regulator was at a concentration of 4 μM and the assay was carried out in the presence of 500 nM calcium. All experiments were repeated at least thrice.

RNA isolated from dissected SCN, SCN cell line or eye were converted into cDNA and used as template to amplify GCAP1, GCAP2, NCALD, HCAL and S100B. GCAP1 is known to modulate the activity of ROSGC1 and ONEGC [81, 86]; GCAP2 modulates the activity of ROSGC1 and ROSGC2 [81]; NCALD activates ROSGC1 and ONEGC in a calcium-dependent fashion [11, 22, 52]; HCAL activates

an unknown CaRGC in the hippocampus [50], and S100B is an activator of ROSGC1, ROSGC2 and ONEGC [81]. Among these NCS proteins, only the GCAPs inhibit the CaRGC activity at high calcium concentrations (micromolar levels) [81]. Neither GCAP was detected in the SCN (Fig. 4.1.3A). On the other hand, all three positive regulators – NCALD, HCAL and S100B – were detected by RT-PCR. Therefore, the calcium-dependent increase in mGC activity in the SCN may be mediated by one or more of these activators. In order to biochemically investigate the possibility, membrane fractions isolated from the SCN were incubated with or without S100B or NCALD (at 4 μM). The cyclase activity was assayed for in the presence of calcium at 100 μM concentration. The results demonstrate that both proteins are able to activate the SCN mGC, with NCALD being a better activator than S100B. No significant stimulation was observed with 4 μM of HCAL under identical conditions (data not shown). Thus, NCALD and S100B are the potential regulators of SCN mGC.

Do the regulators show day – night variations?

If either of these regulators were to play a role in the light entrainment of the SCN mGC, an oscillation in their mRNA levels in response to day-night variations is not unexpected. In order to investigate any variation in the expression of NCALD and S100B, their mRNA levels were assayed by quantitative PCR in RNA samples isolated at different time-points from the SCN 2.2 cells after synchronization. The SCN tissue is comprised of a heterogeneous group of neurons with differential expression of proteins and, presumably, functions. In order to circumvent this drawback, the SCN 2.2 cell line was chosen to analyze rhythmic variations. The SCN

cell line maintains free rhythms, shows responsiveness to glutamate phase-setting and can restore rhythms in animals lesioned for SCN [51, 87-89]. RNA was isolated from SCN 2.2 cells at various time points following synchronization. A number of genes were analyzed in these experiments. The level of L30 mRNA, which is not affected, was used for calibration. The results are presented in the figure below:

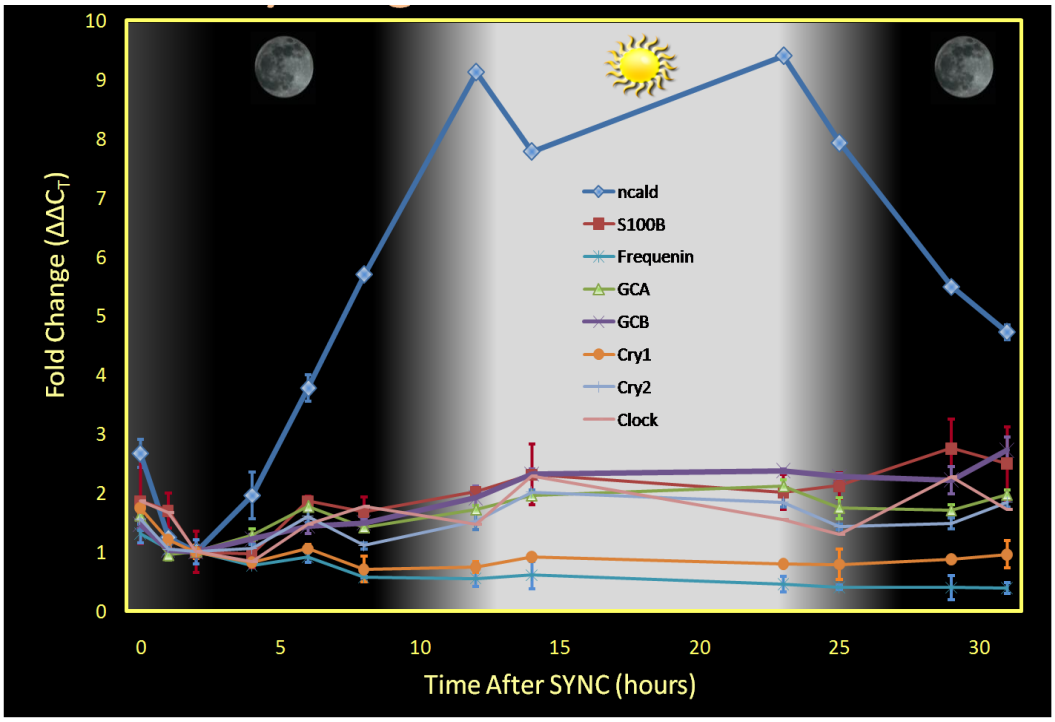

Figure 4.1.4: Robust cycling of NCALD mRNA:

RNA was isolated from SCN 2.2 cells at various time points following synchronization. Real Time PCR analyses were carried out on an ABI 7500 unit using the SYBRgreen dye. All primers produce a single peak upon dissociation curve analysis, indicating a single product without primer dimers or other non-specific products. All primers were shown to be 100% efficient. Analyses of cDNA samples from SCN 2.2 synchronized cells were performed for numerous genes, including neurocalcin δ and S100B. Samples were run in triplicate and their Ct values were averaged. The ΔΔCT value for each gene was calibrated to the L30 level at the corresponding time. Data is presented as fold change in ΔΔ CT values. Data was analyzed using SDS v2.2.2. Standard ΔΔCt values were calculated, with the samples normalized to the 2h time point.

The results (Fig. 4.1.4) clearly demonstrate that the expression of NCALD shows a robust day-night oscillation, with an increase coinciding with the onset of "day" and reaching a peak during "day", followed by a fall in levels. The "day" and "night" times are represented by dark and light backgrounds and the duration of these periods is based on previous studies. A striking oscillation is observed with NCALD mRNA when compared to all other samples (Fig. 4.1.4). As positive controls, Per1 and Clock mRNAs were also analyzed. Almost nine-fold change is observed between 2 h ("night") and 14h ("day") in NCALD mRNA levels. Both Cry1 and Clock exhibit ~2-fold variation, consistent with earlier reports [90]. Similar oscillations are observed in the case of CRY2 and S100B. However, very little variation is detected in the mRNA levels of another NCS protein, frequenin or the two membrane guanylate cyclases: ANFRGC (GCA) and CNPRGC (GCB). Based on the results with CRY1, CRY2 and Clock, it is concluded that the SCN 2.2 were synchronized and in rhythm. Therefore, under these conditions, NCALD exhibits the most variation (~ 9-fold) between "day" and "night", while S100B exhibits some variation (~ 2-fold); on the other hand, little variation is observed in the case of frequenin or either of the membrane guanylate cyclases tested. Thus, NCALD might be one of the most robust oscillators known to date.

In order to investigate if the robust oscillation detected at the mRNA level was also detectable at the protein levels, Western analyses were carried out. The results are presented in figure 4.1.5.

It is seen that the levels of NCALD protein are also in oscillation, with the peak levels during the day, an increase before presumptive "day" and a decrease

before presumptive “night”. Thus, the protein levels follow the mRNA levels during the crucial phase-setting period, before the peak during the “day”. However, there appears to be additional levels of control operating on NCALD expression, since even though the mRNA levels are still higher during the period before “night” (Fig. 4.1.4; NCALD, 25 h), the protein levels approach the baseline (Fig. 4.1.5).

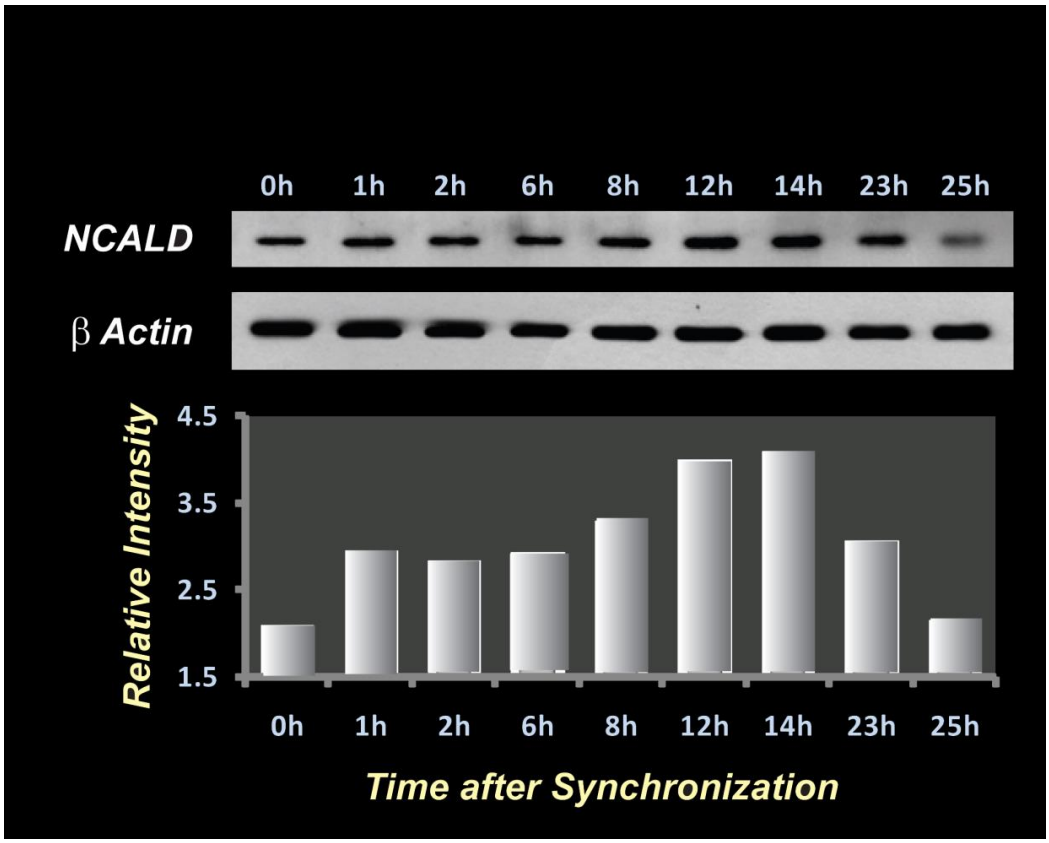

Figure 4.1.5: Oscillation of NCALD protein:
Total protein was isolated from SCN 2.2 cells at various time points following synchronization. The samples correspond to those analyzed for the RNA. After electrophoresis on SDS-polyacrylamide gel, the proteins were transferred to a nitrocellulose membrane and probed with antibodies against NCALD (rabbit) or β-actin (mouse).

Taken together, these results demonstrate that (i) the levels of both NCALD mRNA and protein exhibit day/night variations with the peak during the day and

trough during night; (ii) NCALD expression may be regulated at multiple levels including transcription and translation; and (iii) the mRNA and protein levels are better correlated during “dawn” suggesting pre-dominantly transcriptional regulation. Thus, NCALD could clearly play a role in phase-setting events in response to cellular calcium and could activate mGC in response.

In order to investigate this possibility, synchronized SCN cells were assayed for both mGC activity as well as NCALD mRNA and protein levels during “dawn”. It is evident that the levels of NCALD mRNA closely mirrors the changes observed in mGC activity: decreasing until 2h after synchronization and increasing beyond that to reach a maximum during “day” (Fig. 4.1.6; compare NCALD and mGC activity). Given that elevation of cellular calcium, increased expression of NCALD mRNA and protein and increased mGC activity all occur around this period, it is strongly suggestive that NCALD may regulate the activity of the SCN mGC that is a primary event in phase-setting.

Are the SCN mGCs regulated by NCALD?

It is noteworthy that while mGC activity increases by about 5-fold from “night” to “day”, very little change is observed in the mRNA levels for the two known mGCs in the SCN: ANFRGC and CNPRGC. It is conceivable that either of these cyclases is regulated at the activity level by NCALD or that the NCALD-responsive cyclase is an (as yet) unknown cyclase. In order to investigate if either cyclase could be regulated by NCALD, reconstitution experiments were carried out. Membranes from COS7 cells expressing either ANF-RGC or CNP-RGC were

incubated with incremental concentrations of NCALD in the presence of calcium and guanylate cyclase activity was assayed. The results are presented below.

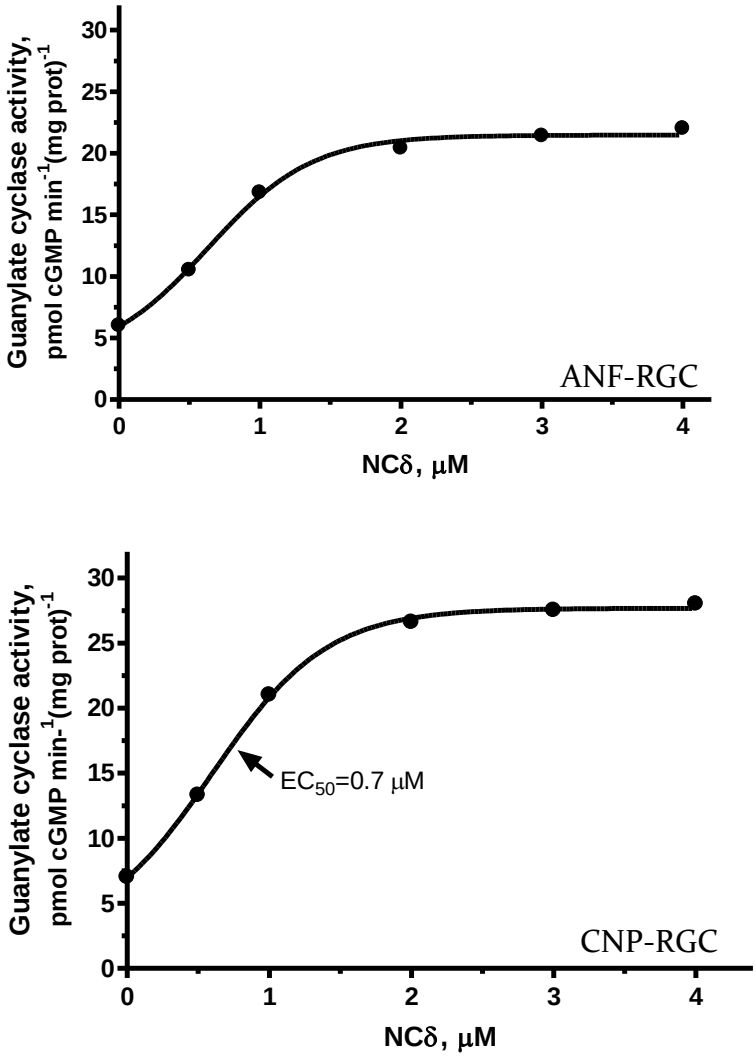

Figure 4.1.6: Both ANF- and CNP-RGCs are regulated by NCALD: Membrane fractions were isolated from COS7 cells individually transfected with either ANF-RGC or CNP-RGC and assayed for guanylate cyclase activity in the presence of incremental NCALD. Results are presented in the respective panels and are from triplicates.

It is evident that both cyclases are stimulated in a dose-dependent fashion by NCALD, with comparable EC_{50} values. Therefore, either or both may contribute to a rise in cGMP through the action of NCALD. Further experimentation was focused on the relevance of NCALD.

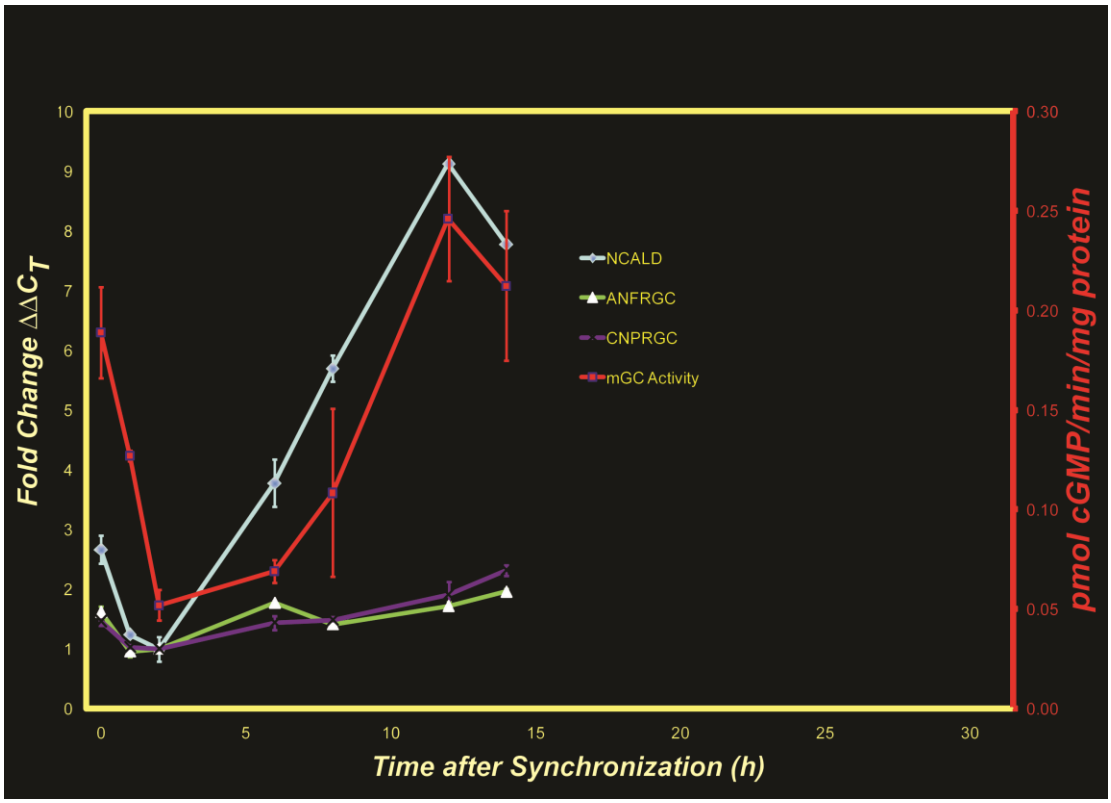

Figure 4.1.7: Oscillation of NCALD protein and correlation to mGC activity: RNA was isolated from SCN 2.2 cells at various time points following synchronization. From duplicate plates, membrane fractions were isolated and assayed for guanylate cyclase activity. Results are from triplicates.

Light, NCALD, mGCs and eye

The next step was to investigate if this linkage between NCALD, light and mGC activity could be demonstrated *in vivo*. The eye was the first choice since SCN is made up of heterogeneous neurons and the expression of NCALD in these

subpopulations remains to be elucidated. On the other hand, NCALD expression in select cells of the retina has been amply demonstrated and its expression has also been shown to occur within a sub-population of ganglion cells [11]. Circadian variation of several molecules expressed in the retina has been documented [91, 92]. Finally, retina is the primary pacemaker for light entrainment of the SCN. In order to determine if NCALD expression in the retina is linked to phase-setting, RNA from the eye was isolated at four different time-points. Both rat and mouse samples were used. Quantitation of the NCALD mRNA and protein was carried out as described before. The results are presented in figure 4.1.8.

It is seen that NCALD protein levels are the highest at 8 AM and lowest at 2 AM. This suggests that the protein levels increase between 2AM and 8 AM – the most critical period for phase-setting. Thus, just as in the SCN 2.2 cells, NCALD expression is elevated in response to "dawn", suggesting a role for phase-setting *in vivo* in the eye. However, unlike the SCN 2.2 cells, a distinct difference is observed in the cycling of the NCALD protein and mRNA levels: in the SCN 2.2 cells, there was very little difference between the two suggesting a tight coupling of transcription and translation; in the eye, on the other hand, the mRNA levels reach maximum before the protein levels (Fig. 4.1.7; Compare mRNA and protein at 2 AM). Thus, regulation at the level of translation may play a critical role in the eye.

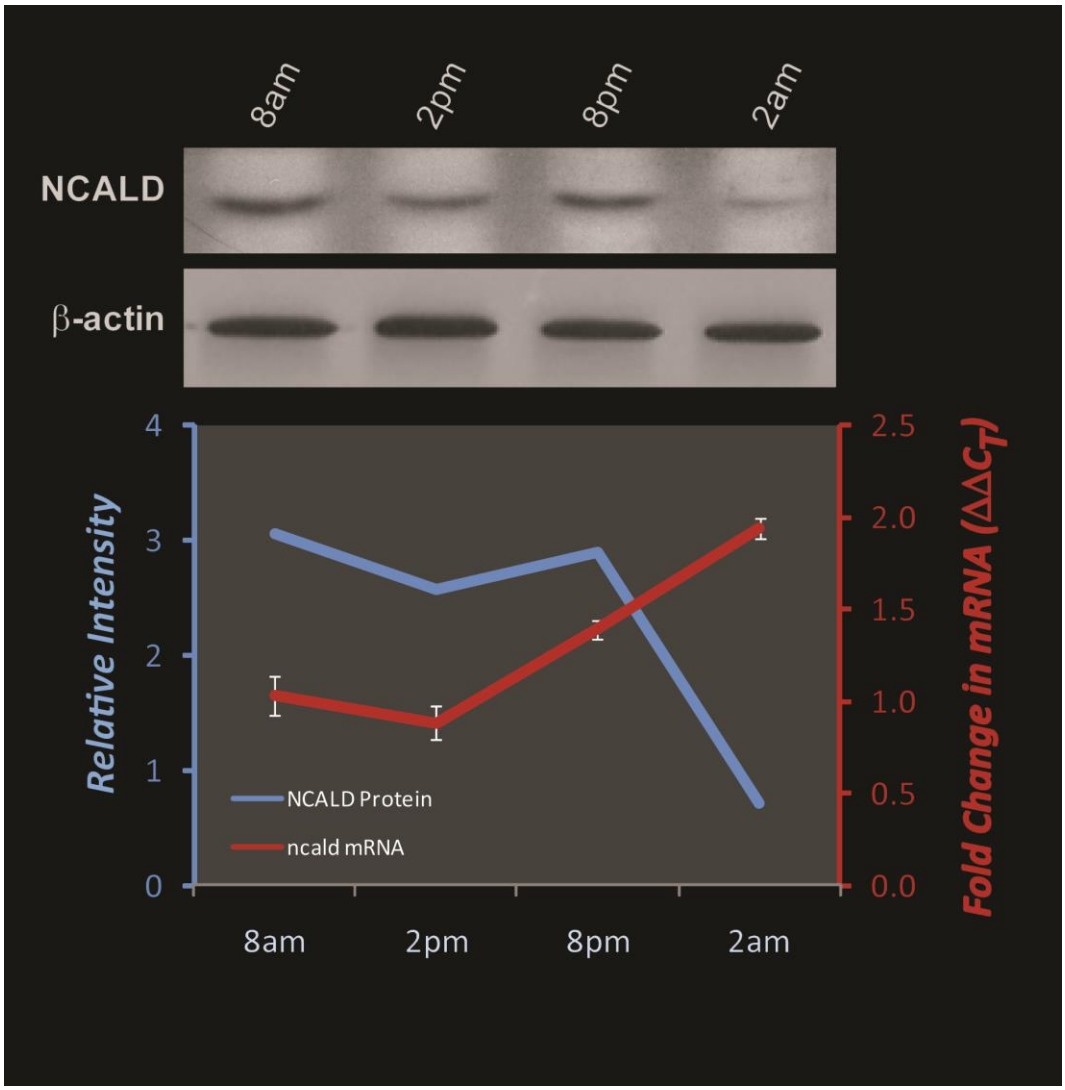

Figure 4.1.8: Oscillation of NCALD protein and mRNA in the rat eye:

Eyes were obtained from euthanized rats at indicated times. RNA and protein were isolated from the samples. NCALD mRNA was assayed through quantitative PCR after reverse transcription using L30 mRNA levels as a standard. NCALD protein was assayed through Western blotting. A representative result from Western blotting is presented in the top panel that depicts NCALD and β-actin protein levels (Control). Relative intensity of the bands was calculated for at least three animals and plotted together with the NCALD mRNA levels in bottom panel. Results are from triplicates.

Skin and NCALD oscillations

Another tissue in which circadian rhythms have been established is the skin [93, 94]. Therefore, it was of interest to investigate if a similar role in phase-setting could be observed for NCALD. Preliminary experiments demonstrated expression of NCALD in multiple cell types of the skin: such as keratinocytes especially the basal cells in the epidermis and muscle and connective tissue components in the dermis. Based on the previous results which argue that NCALD protein levels is the critical regulatory factor and the discovery that NCALD is expressed in multiple cell types in the skin, immunohistochemical analyses were the choice method to investigate NCALD expression in the skin. The tissue was isolated at indicated times, fixed and sectioned. The sections were then stained for NCALD using highly specific antibodies and the presence was detected by Vectastain ABC kit followed by peroxidase staining. Expression of NCALD results in a brown stain. As a control, the sections were also stained for an unrelated protein – vimentin. The results are presented below:

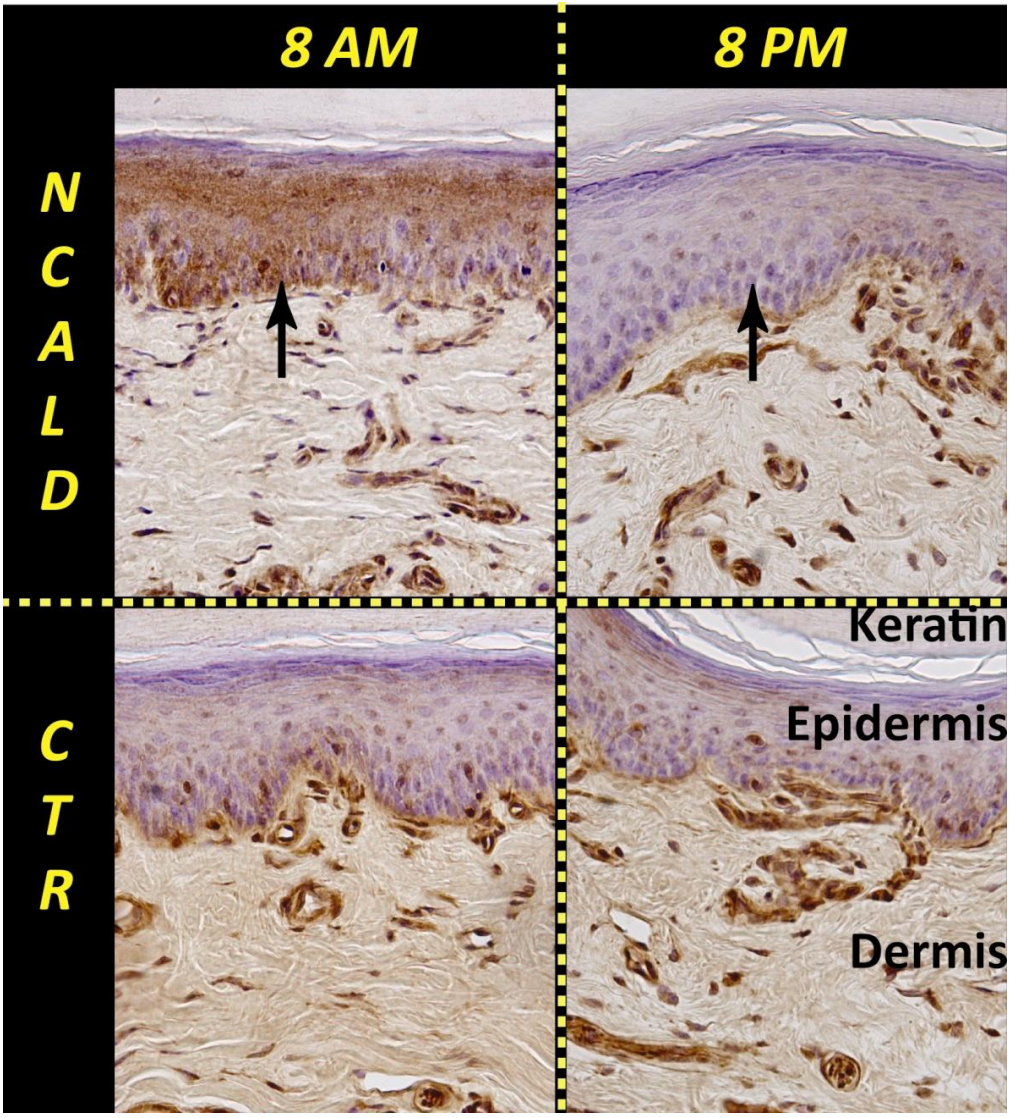

Figure 4.1.9: Oscillation of NCALD protein in the rat skin:
Sections of the skin were stained with antibodies against NCALD (Panel NCALD) or vimentin (Panel CTR – control). Positive reaction appears as a brown color. In the NCALD panel, arrow indicates basal keratinocytes, which express NCALD at high levels. The keratin layer, epidermis and dermis are labeled.

It is evident that higher expression of NCALD is observed in the keratinocytes at 8 AM when compared to 8 PM. The results are consistent with those obtained earlier, and argue for a role for NCALD in setting the phase in response to light. It is

noted that this function appears to be restricted to the keratinocytes in the epidermis. While NCALD expression is observed in multiple layers and cell types, the variation over time is observed is observed almost exclusively in the keratinocytes. No variations are observed when the sections are stained for vimentin, a protein that is expressed in the neurovascular bundles.

Conclusions:

1. Both SCN tissue and the SCN 2.2 cell line express components of mGC signaling pathway.
2. NCALD mRNA exhibits a robust circadian rhythm in SCN 2.2 cells.
3. mGC activity correlates with NCALD mRNA/protein levels during phase-setting.
4. NCALD cycling occurs in tissues and is consistent with a role in phase-setting.

4.2: NCALD serves as a chaperone for S100B

In the previous chapter, cycling of NCALD and S100B mRNA and proteins were demonstrated. In this section, we demonstrate that NCALD and S100B specifically interact *in vitro*. We further identify that the EF1 hand of NCALD is essential for the interaction. Using Bimolecular Fluorescence Complementation (BiFC) assay, specific interaction of S100B with NCALD *in vivo* is demonstrated in COS7 cells. Upon treatment with histamine (which elevates cellular calcium), the NCALD-S100B complex translocates to the vesicle-rich, perinuclear region; however, S100B by itself does not exhibit this movement. It is further demonstrated a similar translocation is also observed with HPCA-S100B complex, albeit with a different kinetics.

Introduction

NCS proteins play a crucial role in mediating Ca^{2+} signaling. They are highly expressed in neurons and bind to calcium through EF hand motifs. Most NCS proteins can become membrane-associated by using N-terminal myristoylation group [reviewed in: [16]]. Numerous NCS proteins have been identified in vertebrates, including S-modulin, visinin, frequenin, hippocalcin, VILIP (Visinin-like Proteins), and multiple isoforms of neurocalcins [17]. In this study, we investigate the interaction between two proteins that contribute to circadian rhythm: NCALD and S100B.

NCALD is primarily expressed in the central nervous system, spinal cord, retina, inner ear, olfactory epithelium and zona glomerulosa of the adrenal gland [17, 18]. It consists of four EF hands although EF1 hand is disabled from binding calcium. A major feature NCALD is N-terminal myristoylation, which allows NCALD to interact with cell membrane. The myristoyl group is sequestered in the Ca^{2+} free state. When it binds to Ca^{2+}, the myristoyl group extrudes, allowing it to interact with membrane [18, 19]. Upon the elevation of intracellular Ca^{2+}, NCALD is translocated to the perinuclear compartment from cytosol [95]. Regarding the role of NCALD in photic entrainment: (i) it is known to stimulate mGC in a calcium-dependent fashion [10] (ii) NCALD expression has been localized to subset of SCN neurons that interface with the RHT [21]; (iii) Additionally, NCALD is expressed in the retina in many species in a subpopulation of ganglion cells that may be the non-visual photoreceptors critical for entrainment [22].

The S100 proteins are a group of proteins which consist of at least 25 members in human, including S100B. The proteins are dimeric, having two "EF-hand" calcium binding motifs in each subunit. Most S100 proteins can bind calcium and undergo a conformational change which allows them to control cellular activity by interacting with other proteins [reviewed in: [23]]. It has been suggested that S100B is one of the target proteins of NCALD and that the S100B-NCALD complex may be involved in Ca^{2+} signaling in the glial cell [24]. Therefore, it was of interest to determine if NCALD and S100B bind and if they did, whether the binding contributed to cellular response to calcium signals.

Materials and Methods:

Described in Section 3.

Results

NCALD and S100B interact *in vitro*.

Purified proteins were used for *in vitro* binding assays through membrane overlay. HPCA is another neuronal calcium sensor protein, which shares an 88% identity (95% similarity) with NCALD. Unlike NCALD, HPCA does not exhibit a light-dependent variation in either SCN cell line or animal systems. Therefore, HPCA was also used to test binding. Ovalbumin was used as the negative control.
The results are presented in Fig. 4.2.1.

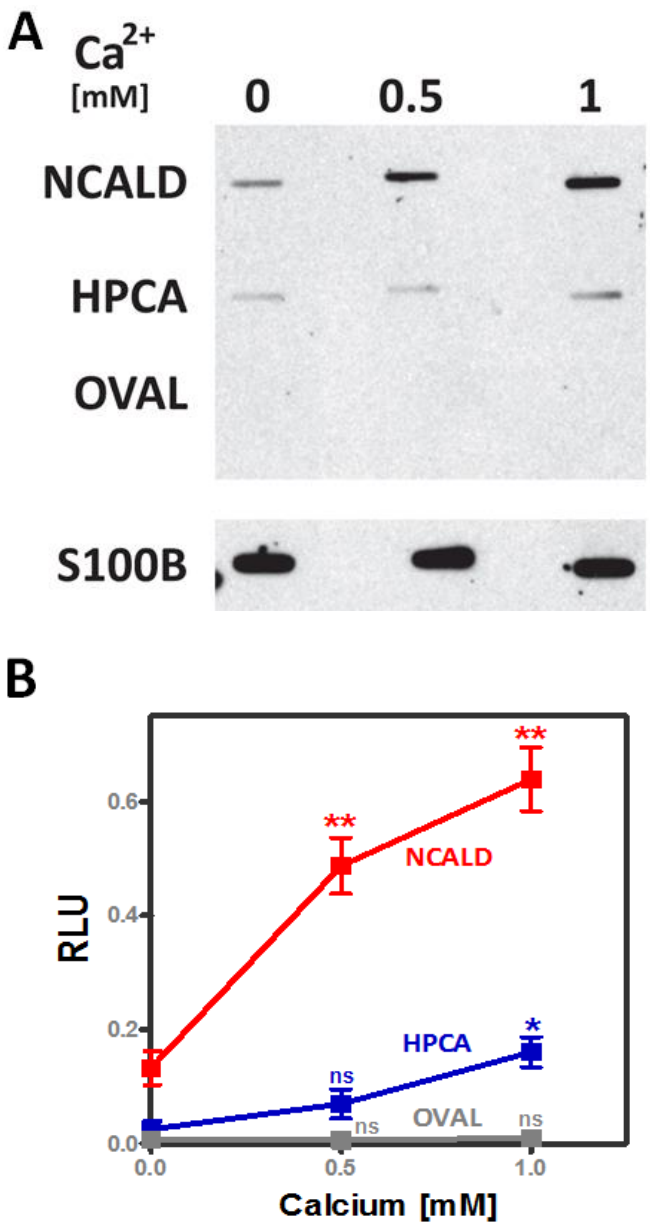

Fig.4.2.1 NCALD binds to S100B *in vitro*

(A) Purified NCALD, HPCA and commercial OVAL were spotted onto nitrocellulose and the membrane was then incubated with S100B in the presence of indicated concentrations of $CaCl_2$. After 1hr incubation, the blot was washed with the buffer. Bound S100B was detected using its antibody following standard western blotting protocol and ECL detection. **(B)** Intensity for each band was measured using imageJ and then plotted in Prism.

The results suggest that NCALD binds to S100B, while HPCA does not bind as well. Ovalbumin does not bind to S100B. Optimal binding for NCALD and S100B requires calcium.

NCALD Binding to S100B requires EF1 hand

To investigate the binding site, we created chimeric proteins: NCHC and HCNC. NCHC contains the N-terminal region of NCALD up to and including the EF1 hand with the rest of the region from HPCA; HCNC contains the N-terminal region of HPCA up to and including the EF1 hand and the rest of the region from NCALD. Purified NCHC and HCNC were tested in membrane overlay. The membrane overlay results showed (Fig. 4.2.2A) that NCHC binds to S100B while HCNC does not, which suggests that the EF hand 1 constitutes the binding site for NCALD and S100B.

Previous data from our laboratory show that EF1 region is responsible for the type of change in the protein structure induced by calcium binding. To further expand on the idea that the non-calcium binding EF-1 region may be responsible for the binding, more mutants were then created. NCALD has two conserved tryptophan residues – one at position 30 and another at position 103. The tryptophan at position 30 is located in the non-calcium binding EF1 hand. While the second at position 103, is in EF hand 3. The crystal structure suggests that W30 is involved in stacking interactions with other hydrophobic amino acids. These tryptophan residues were mutated to phenylalanine. The membrane overlay results showed (Fig. 4.2.2B) NCALDW30F abolished the binding while NCALDW103F binds as well as wt NCALD, which suggests that the tryptophan at position 30 is critical for this binding.

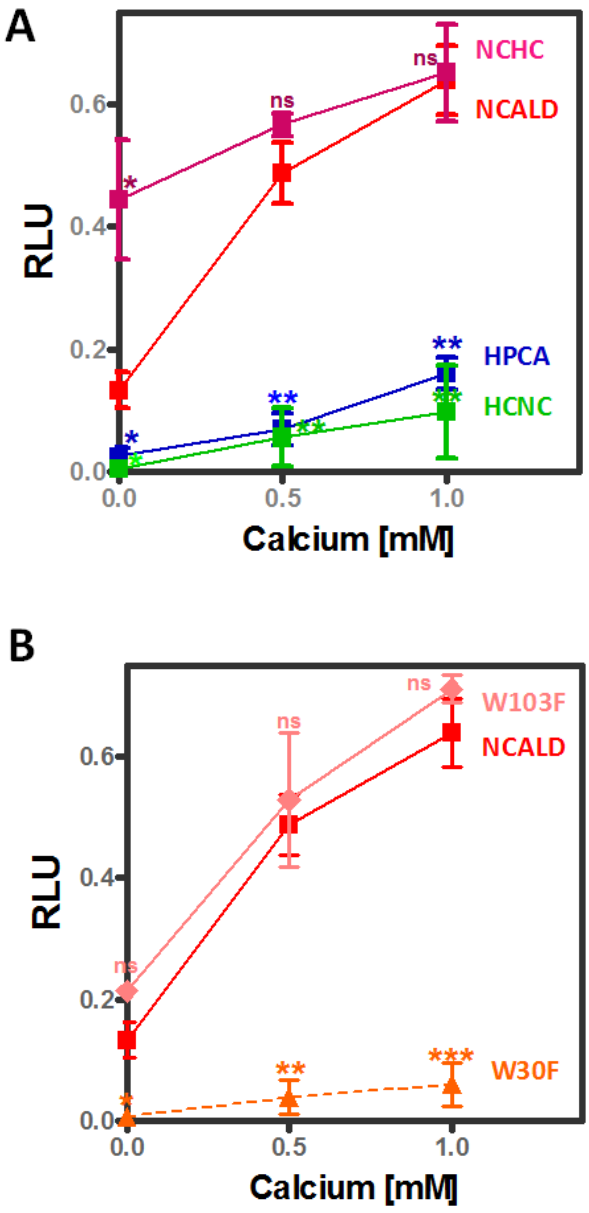

Fig.4.2.2 EF1 region of NCALD is necessary for the binding to S100B *in vitro*

Purified NCHC, HCNC **(A)**, NCALDW30F and NCALDW103F **(B)** were spotted onto nitrocellulose and the membrane was then incubated with S100B in the presence of indicated concentrations of $CaCl_2$. Bound S100B was detected using its antibody following standard western blotting protocol and ECL detection.

NCALD and S100B interact *in vivo*.

The results presented above show that NCALD and S100B specifically interact s and the interaction requires the EF1 hand of NCALD. The next step was to investigate if the interaction occurred *in vivo*. Bimolecular fluorescence complementation (BiFC) is one of the newer approaches. It is based on the tagging two interacting proteins with half of a fluorescent protein (FP) each. Upon the interaction of the putative binding partners, the two halves of the fluorescent protein are brought closer, which enables them to associate with each other to form the 3-D structure and fluoresce [96]. In order to investigate the interaction between NCALD and S100B, we fused NCALD and S100B with YFP 1-158(YN) and YFP 159-238(YC) respectively. Co-transfection of COS 7 cells with NCALD-YN-pcDNA1 and YC-S100B-pcDNA1 generated fluorescent signal while transfection of individual constructs alone did not generate fluorescent signal (Fig4.2.3A). The active form of S100B is known as a dimer. Therefore, we fused S100B with YFP 1-158(YN) and YFP 159-238(YC) and transfected the two constructs into COS7 cells. The co-transfection with S100B-YN and YC-S100B into COS7 cells also generated fluorescent signal. Multiple negative controls including S100B-YN, YC-S100B, NCALD-YN, YN&S100B-YC, NCALD-YN&YC and YN&YC vectors by themselves were also tested for restoration of fluorescence. The results are plotted in Fig 4.2.3B.

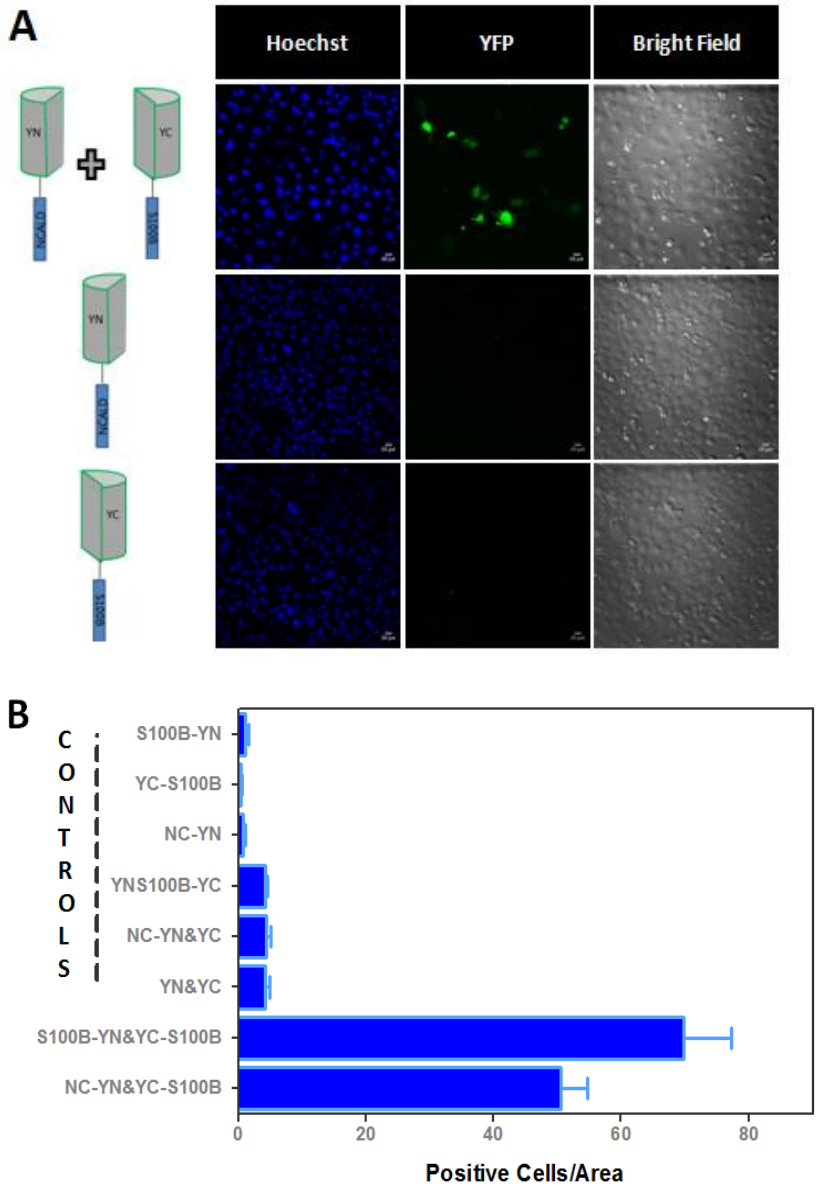

Fig 4.2.3. NCALD and S100B bind in vivo

COS 7 cells were co- transfected with constructs NCALD-YN-pcDNA1 and YC-S100B-pcDNA1. Co-transfection of S100B-YN and YC-S100B served as positive control while negative controls include transfection of S100B-YN, YC-S100B, NCALD-YN, YN&S100B-YC, NCALD-YN&YC and YN&YC. **A**. Cells were monitored using Nikon Confocal microscope 48 hours after transfection. **B**. Positive cells numbers per area were plotted in prism.

Translocation of the complexes

N-myristoylation is a characteristic feature of NCS proteins. The myristoyl group allows for the interaction with hydrophobic fragments, which facilitates translocation from cytosol to membrane fractions [97-99]. It has been demonstrated that the translocation of HPCA in hippocampal neurons plays a physiological role in Ca^{2+}-dependent local activation of specific molecular targets [100].

To investigate if the complexes- NCALD-S100B, HPCA-S100B and S100B-S100B - translocate in the cell in response to elevated calcium, histamine was used to elevate the intracellular calcium levels. The location of the complexes was detected by fluorescence. Under normal conditions, fluorescence was found diffused throughout the cell. When histamine was added, NCALD-S100B and HPCA-S100B complexes translocated and localized within a specific region of the cell within 5 min of addition. With time, the fluorescence gradually diffused back to its ground state. However, no significant movement was observable upon histamine addition in cells transfected with S100B-S100B complex.

Even though both NCALD-S100B complex and HCPA-S100B complex translocate to the same region of the cell, we found that the kinetics of the two were different. Upon analysis of the translocation kinetics, we found that NCALD-S100B complex stays at the perinuclear region substantially longer than HPCA-S100B complex. The result suggests a higher sensitivity to calcium and higher affinity to the membrane fraction for NCALD than HPCA (Fig.4.2.4).

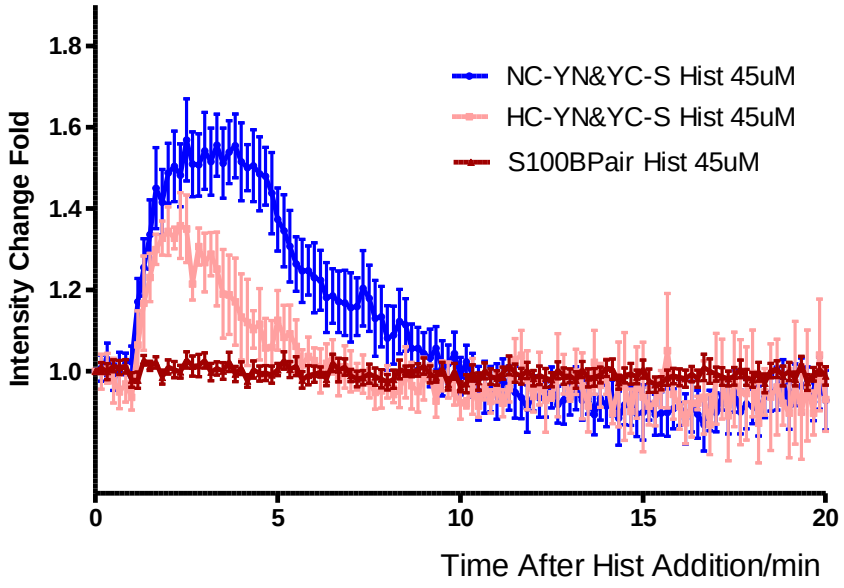

Fig.4.2.4 Translocation kinetics of BiFC complexes

Determination of change in fluorescent intensities as a function of time: Readings from replicate experiments were averaged and the mean is presented from the perinuclear region of cells transfected with YN-NCALD and S100B-YC(blue line); YN-HPCA and S100B-YC (pink lines) and YN-S100B and S100B-YC(red line).

Discussion

In this report, we demonstrate a direct interaction between NCALD and S100B both *in vitro* and *in vivo* and identify that the NCALD EF1 hand is essential for this interaction. The finding that NCALD-S100B complex translocates while S100B-S100B does not translocate suggests that NCALD serves as a chaperone for S100B.

The Neuronal calcium sensor proteins are responsible for calcium related signal transduction. It is crucial for a cell to sense different level of calcium, even

negative changes in calcium concentrations. NCS proteins can sense the change resulting in a conformational change followed by movement to different location(s) inside the cell and binding with a wide range of partners.

However, the NCS family is a highly conserved family, which raise the question that why many similar NCS proteins are needed during evolution. In this study, we demonstrate the different kinetics of translocation between NCALD and HPCA suggest a mechanism of how a cell senses different levels of calcium and respond differently by expressing either NCALD or HPCA, or both together.

4.3: Translocation of Hippocalcin in vivo in response to histamine: a comparative analysis of two approaches for quantification-using ImageJ – an open-source software

The purpose of this study is to compare two methods of fluorescence intensity estimation as a function of time to track the translocation of HPCA in COS7 cells upon histamine addition. A line method or area method was used to measure the fluorescence intensities in two sets of COS cells. The results were then compared by curve-fitting and statistical analyses.

INTRODUCTION

Proteins are known to shuttle among different subcellular destinations to perform various functions. Monitoring translocation, therefore, is important in understanding protein function. Traditional approaches have relied on biochemical methods to measure protein levels in various cellular compartments over time (e.g. western blotting subcellular fractions at sequential time points). While these approaches have produced significant advances in elucidating molecular mechanisms of protein function, they also have limitations. For example, they are not suitable for tracking protein translocation in single cells, limiting kinetic analysis to populations of cells. They also have limited time resolution due to tissue destruction required for biochemical assays at each time point. In addition, protein localization may be sensitive to the concentration of cytosolic ions and metabolites that are likely to be lost during the fractionation procedure.

The development of techniques to label proteins with genetically-encoded fluorescent tags, combined with advances in live cell fluorescent microscopy, has circumvented many of these limitations. They permit direct visualization of biochemical processes in living cells in real–time. A current challenge is to couple image processing techniques with statistical and computational tools to interpret and extract quantitative information from the vast amounts of unstructured image data generated by time-lapse imaging experiments.

Here we demonstrate a reliable and easy-to-implement quantitative image processing method to assess protein translocation between subcellular compartments

in living cells, based on the computation of the spatial variance of time-lapse microscope images. To develop the method, we chose to study the neuronal calcium sensor protein HPCA, which has been demonstrated to translocate to the trans-Golgi network upon elevation of cellular calcium [101-103]. We then measured translocation between intracellular compartments as ratio of fluorescence intensity between two user-defined intracellular regions of interest (ROI) in microscopy images. Two different approaches were used to select the ROIs using the different functionalities available in FIJI – ImageJ [48]. The results were then compared using statistical packages.

Materials and Methods

Described in Section 3

Results and Discussion

1. Translocation of HPCA to perinuclear region upon histamine addition – analyses by line method.

   To investigate the localization and behavior of HPCA, the coding region was conjugated to YFP (HPCA-EYFP-pcDNA3) and the construct was transfected into COS-7 cells as described in the Materials and Methods section. Unconjugated YFP (EYFP-pcDNA3, vector alone) served as a control. Histamine was used to elevate the intracellular calcium levels. Under normal conditions, fluorescence in cells – whether transfected with conjugated or control constructs – was found to be diffused throughout the cell (Fig 4.3.1A and 4.3.1D). After histamine addition, HPCA-conjugated EYFP translocated and localized within a specific region of the cell by 5 min after addition (Fig 4.3.1B). With time, the

fluorescence automatically diffused to its ground state (Fig. 4.3.1C). However, no significant movement was observable upon histamine addition in cells transfected with unconjugated vector alone (Fig 4.3.1D-F).

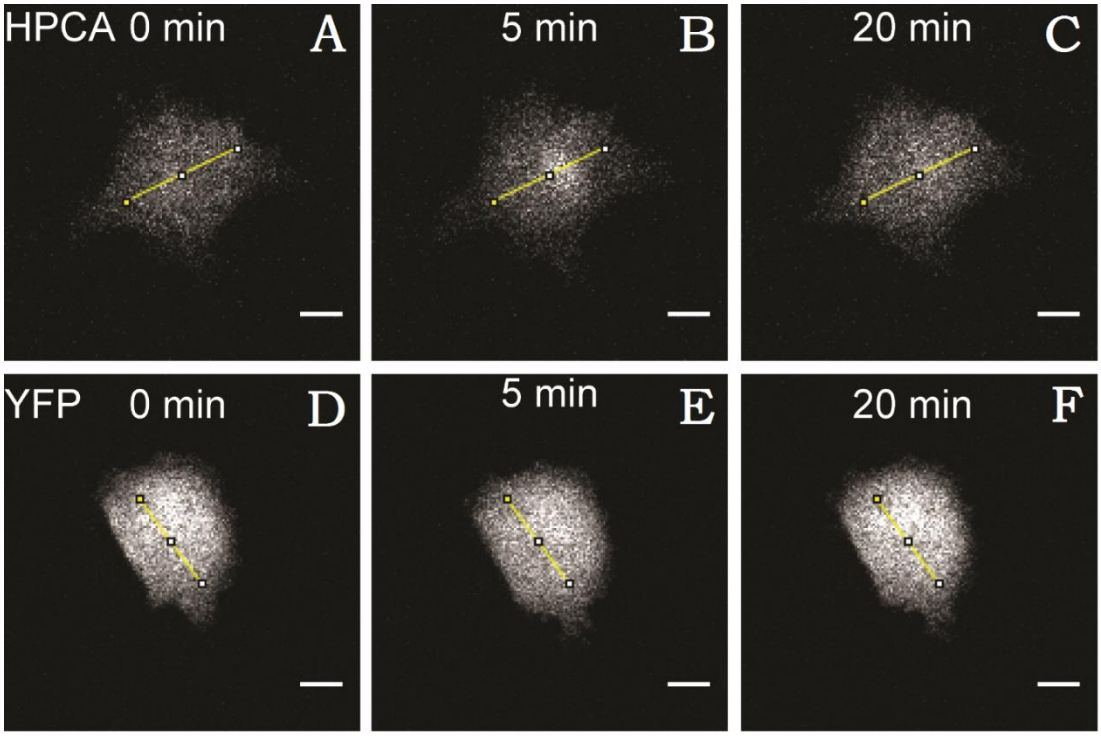

Figure 4.3.1: Fluorescent vectors carrying YFP alone (YFP) or YFP fused to Hippocalcin (HPCA) were transfected into COS7 cells and imaging was carried out 24-36 hours after transfection as described in Materials and Methods. Live images were obtained every 10 seconds and were obtained for at least for 20 min after histamine addition to the cells. Representative images are presented above at 0, 10, and 20 min after histamine addition to YFP- or HPCA-transfected cells. The line used for measurement is depicted in yellow.

As a first step towards quantifying the translocation, a line was drawn across each cell that included the change in fluorescence when observable. The line would cover the nuclear region, membrane-rich perinuclear region and the rest of cytosol (indicated in yellow, Fig 4.3.1A-F). Fluorescence intensity was measured for each

pixel along the line at each time instance, before and after histamine addition. Measurement was carried out for both YFP and Hoechst (used to stain nuclei) along the line. To identify the region with maximal change in fluorescent intensity measurements relative to the nucleus, the reading of Hoechst staining was overlaid with that for YFP (Fig. 4.3.2A). The region of maximal change, where HPCA-EYFP concentrated in the cell, is the perinuclear area. The finding is consistent with previous studies in Hela cells [103]. The raw fluorescent intensity readings from every pixel within this region (19-28 in the representative cell) were then obtained, corrected for noise and plotted as a function of time. The values from all the pixels were then averaged and the mean is presented in figure 2C. Similar analyses were carried out with several cells transfected with the conjugated vector (HPCA) or unconjugated vector only (Vector) and the resultant curves are presented in figure 4.3.2D. Significant changes were observed only with HPCA: HPCA translocated to the perinuclear region within 5 min after histamine addition and then slowly diffused away over the next 15 min. No significant change was observed with vector alone.

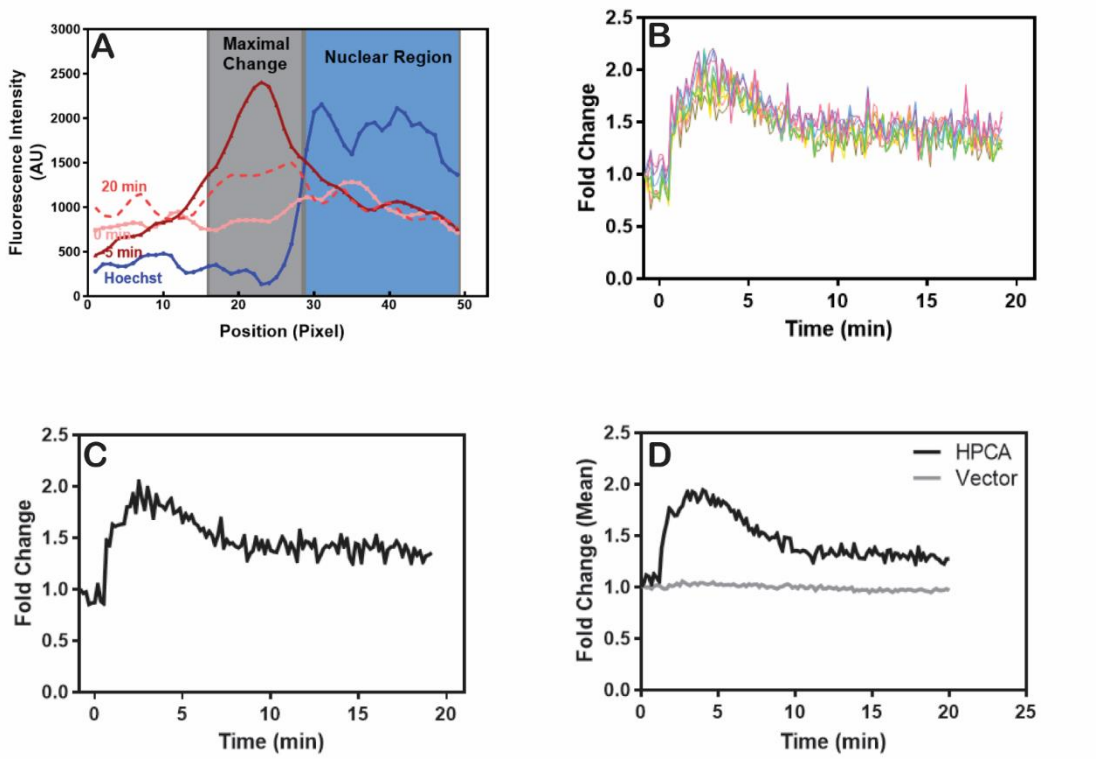

Figure 4.3.2: Determination of change in Fluorescent intensities as a function of time:

(A) Fluorescent intensities across the line from 0,5 and 20 minutes were plotted and were overlaid with that for Hoechst staining and the pixel positions depicting maximal change in intensity over time were chosen; (B) Variations in fluorescence in those positions were plotted as a function of time (n=6) as fold change over time 0; (C) The mean change in fluorescent intensity was plotted as a function of time; (D) Readings from replicate experiments were averaged and the mean is presented from the perinuclear region and nuclear region for cells transfected with HPCA (black lines) and for the perinuclear region for cells transfected with the vector alone (gray line).

While reproducible results are obtained with this method and the conclusions are consistent with earlier studies, the location of the line varied from cell to cell and is dependent upon visual examination of the image. Therefore, an alternate method

was devised using tools available within ImageJ that could be applied to all images more uniformly.

2. Translocation of HPCA to perinuclear region upon histamine addition – analyses by area method.

To measure the amount of hippocalcin at the subcellular level and its response to histamine, an area tool was utilized to select the regions of interests (ROIs). The representative results are shown in Fig. 4.3.3. The granule-enriched elevated perinuclear area can be viewed clearly in the DIC image and were circled using the Freehand Selection tool solely based on the DIC images (marked by a yellow boundary) in both YFP-HPCA transfected cells (Fig. 4.3.3A) and YFP-only transfected cells (Fig. 4.3.3E). These were the regions of interest (ROI). The ROIs were saved and applied to the images to measure the fluorescent intensity within the selected ROI across time (Fig. 4.3.3B-23 & 4.3.3G-3I) using a Multi-Measure tool. The result obtained from the representative cells was plotted in Fig. 4.3.2I & 4.3.2J. Upon histamine addition, a sharp increase in the fluorescent intensity followed by a gradual decrease within the tested ROIs was detected in the YFP-HPCA transfected cells, which indicates a translocation of hippocalcin into the ROI. However, in the YFP-transfected cell, the fluorescent intensity from the ROIs stayed comparably similar during the observed time frame (50 seconds before adding histamine to 20 minutes after the addition). Similar analyses were carried out with several cells over replicate experiments and the mean is presented in figure 4.3.3K. In cells transfected with HPCA conjugated with YFP, a fast accumulation within the ROI upon histamine

addition, followed by dissipation is observed (Fig. 4.3.3K; HPCA); no such increase is observed in cells transfected with the vector control (Fig. 4.3.3K; Vector).

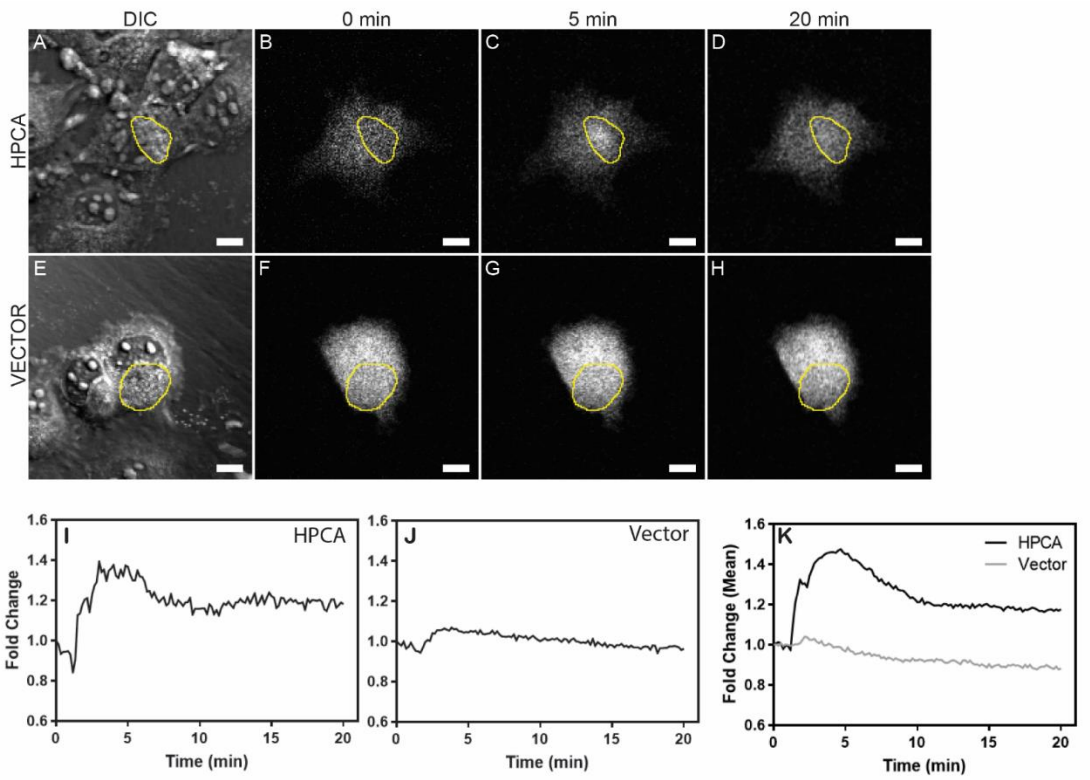

Figure 4.3.3: Determination of translocation using the Region of Interest method:

Live images were obtained every 10 seconds and were obtained for at least for 20 min after histamine addition to the cells as described earlier. The high-contrast vesicle-rich region near the nucleus was identified through DIC imaging and the region of interest (ROI) was then used to assess fluorescence. Representative DIC images as well as fluorescent images at 0, 5, and 20 min after histamine addition are presented for cells transfected with HPCA-YFP (HPCA) [Panels A through D] or YFP alone (VECTOR) [Panels E through H]. The boundary of the ROI is marked by a yellow line. The fold change in fluorescent intensity within the ROI as a function of time within the single presented cell transfected with HPCA (Panel I) or Vector alone (Panel J). Similar measurements from multiple cells over two experiments (n=7) were used to calculate the mean and is presented in Panel K.

3. Fitting curves and comparison of the two methods:

The mean fluorescent intensity measurements for each sample of seven COS-7 cells were recorded for 121 times ranging from 0 to 20 min. The mean values across each of the 121 time intervals for the seven COS-7 cells were next calculated independently for each sample. The mean total intensity for all of the line method estimates was 1.45 (SD = 0.23), and the mean total intensity for all of the area method estimates was 1.25 (SD = 0.12), Welch's t' (178) = 8.74, Cohen's d = 1.09, P < .001. The mean intensity measurement estimated by the line method was thus significantly higher than the mean intensity measurement estimated by the area method. This observation is consistent with the fact that the line is drawn subjectively based on observable intensity differences.

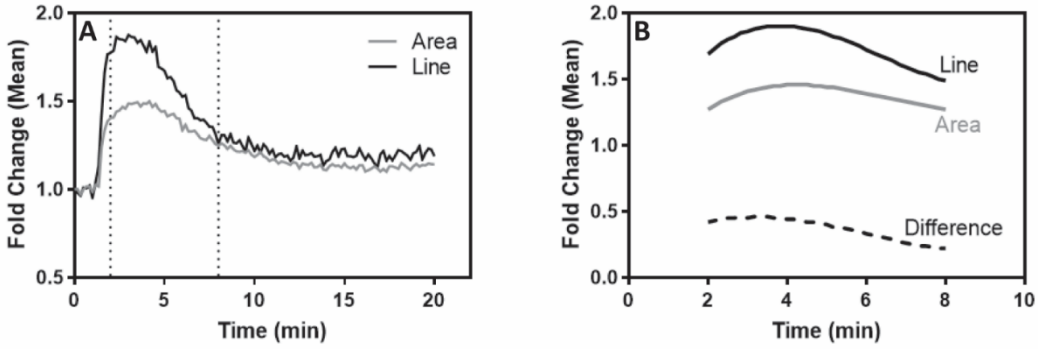

Figure 4.3.4: Comparison of the line and Region of Interest method and curve fitting analyses:

Mean of data obtained from multiple experiments using the two methods are presented together in Figure 4.3.4A. Mean of data after the curve-fitting analyses are presented in figure 4.3.4B, along with the difference between the two. The curves span from 2 minutes to 8 minutes, when they are stable. Dotted lines indicate the duration in figure 4.3.4A.

The curves plotted for the area and the line method (Fig. 4.3.4A, reproduced from figures 2 and 3) along with a visual inspection of the plots for the 121 line and

area method mean intensities with respect to time suggested that the histamine response curves for both methods were similar. A product-moment correlation was calculated between the 121 mean intensity values for both methods to determine the magnitude of the similarity between the curve shapes. The significant correlation was 0.95, $P < .001$, indicating high similarity and suggesting that both line and area methods might be reflecting similar curves over time. However, inspection of the mean values for both methods indicated that the mean intensity values did not start to stabilize until two minutes or more had elapsed and that the mean intensity values leveled off after 8 minutes. Regression analyses were thus restricted to mean intensity values from 2 to 8 min (indicated by dotted lines in Fig. 4.3.4A) to yield more precise estimates, and cubic regression models were subsequently found to fit the curves best, i. e., explain the most variance. The cubic equation for the line method is: 0.709 X min – 0.133 Min X Min + 0.007 X Min X Min X Min + 0.74 [R2 =0 .92, F (3, 33) = 122.20, P < .001], and the cubic equation for the area method is: 0.454 X min -0.079 X Min X Min + 0.004X Min X Min X Min + 0.648 [R2 =0 .97, F (3, 33) = 122.20, P < .001].

Figure 4B shows the estimated cubic curves for the line and area methods along with a curve representing the mean differences between the curves which was calculated by subtracting the cubic regression mean estimates for the area method from those for the line method.

The curves displayed in Figure 4.3.4B indicate that the maximum, mean intensity value for the line method occurred at 3.5 min, whereas the maximum intensity for the area method began at 4 min. The mean time until maxima (1.90) for

the 26 times from 0 to 1.90 for the line method was 2.08 (SD = 1.28) min, whereas the mean time until maxima for the 28 times from 0 to 1.46 for the area method was 2.25 (SD = 1.37) min, t (52) =.46, ns. The times are comparable. Given that histamine addition occurred at 1 min, the mean time until maxima are 1.08 min and 1.25 min for the line and area methods respectively. These are in line with the times reported from an earlier study [95].

The mean fluorescent intensity measurements for each sample of seven COS-7 cells were recorded for 121 times ranging from 0 to 20 min. The mean values across each of the 121 time intervals for the seven COS-7 cells were next calculated independently for each sample. The mean total intensity for all of the 121 line method estimates was 1.45 (SD = 0.23), and the mean total intensity for all of the 121 area method estimates was 1.25 (SD = 0.12), Welch's t' (178) = 8.74, Cohen's d = 1.09, $P < .001$. The mean intensity measurement estimated by the line method was thus significantly higher than the mean intensity measurement estimated by the area method. However, the standard deviations and thus variances for the two methods were statistically different, $F=58.05$, $P<0.001$. The standard deviation for the line method was twice as that for the area method. The area method, predictably, yielded less variable measurements because there was no subjective estimate needed for the line placement. Thus, a more objective choice of the ROI is possible using a judicious combination of filters in ImageJ. While the user-defined line method is comparable in results obtained, it is tainted by subjectivity. Development of the method, it is hoped, will lead to automated analyses of a large number of images.

4.4 Altered calcium response of two critical mutations in Hippocalcin which cause autosomal recessive dystonia

It was demonstrated that both NCALD and HPCA exhibit calcium-invoked translocation and ferry S100B also, albeit with different kinetics in cells. Is the ability of NCS proteins to translocate to specific cellular locations upon change in calcium levels a critical aspect of signal transduction? An opportunity to address this question was provided by the discovery that two mutations in the HPCA gene are linked to autosomal recessive primary-isolated dystonia [28]. We demonstrate that it is not the binding ability but the sensitivity that has been altered by the mutations, compromising the signaling transduction ability.

Introduction:

The neuromuscular movement disorder Dystonia is characterized by repetitive movements and tremors. Charlesworth et al [104] identified two critical mutations in Hippocalcin which caused the autosomal recessive primary isolated dystonia, or type two dystonia. The authors first identified a family that had inherited Dystonia in an autosomal recessive manner. The family's genes were sequenced and a single mutation was identified. The gene that was affected was the Neuronal Calcium Sensor protein Hippocalcin (HPCA) containing an N75K point mutation. The authors then searched a database of people suffering with dystonia and found another patient who also had a mutation in HPCA, specifically T71N.

HPCA is a Neuronal calcium sensor protein, a family which is characterized by 4 EF-hand motifs which are helix-loop-helix structures that bind calcium [105]. The EF hands are distributed between the N and C-terminal lobes of the protein. EF-1 and EF-2 are located in the N-terminal half of this protein, while EF-3 and EF-4 are in the C-terminal half of the protein [97]. For most of the NCS members, EF-2-4 bind calcium, while EF-1 is non-functional with respect to binding calcium, due to a conserved Cys-Pro mutation. In addition HPCA has a covalently linked myristoyl group which allows for the interaction with lipid bilayers, and facilitates interaction with other membrane proteins [99]. This myristoylated N-terminus facilitates the translocation from the cytosol to the membrane [97, 98], and has been demonstrated to be critical for targeting NCS proteins to specific membrane locations [101, 106]. In this manner, the modification allows the proteins to respond spatially to a calcium signal.

Previously, HPCA has been demonstrated to be critical for long term potentiation of memory (LTP); because mice that lack HPCA function have demonstrated impaired long-term memory [26], visual learning, and creation of spatial memories [27]. Biochemically, HPCA interacts with potassium channels to modulate hyperpolarization of contributing to long-term potentiation LTP [25, 107]. HPCA has been shown to interact with the mGCs, Olfactory Neuron-Epithelial Guanylate Cyclase (ONE-GC) [50, 108] and Rod Outer Segment Membrane Guanylate Cyclase type 1 (ROS-GC1) [22]. HPCA activates these partners in a calcium-dependent manner.

Both of these mutations in the HPCA gene are located in the calcium-binding EF-2 hand. Based on the positions and location of the mutation, the authors concluded that HPCA in dystonia patients would be rendered non-functional. The authors came to this conclusion because the EF-2 is one of the critical calcium binding EF hands. Both mutant HPCA expressed in these patients would still contain 2 functional EF hands, which should still bind calcium even if the EF-2 hand was rendered inoperable. The two mutations are likely to cause minimally different effects on HPCA. Both mutations are in the EF-2 binding hand. Thr 71 is not directly involved in calcium binding. The mutation to Asn, another polar, uncharged residue is not a great change. However, the Asn at 75 is directly involved in the coordination of calcium binding in the EF-2. The mutation to the positively charged Lys could potentially interfere with calcium binding, possibly knocking out the calcium binding in the EF-2 hand.

We hypothesize that the HPCA proteins still function, however, at a reduced capacity.

Materials and Methods:

Described in Section 3.

Results:

The neuromuscular movement disorder Dystonia is characterized by repetitive movements and tremors. In the paper by Charlesworth et al [104], the authors identified two critical mutations in hippocalcin which caused the autosomal recessive primary isolated dystonia, or type 2 dystonia. The authors first identified a family that had inherited dystonia in an autosomal recessive manner. The family's genes were sequenced and a single mutation was identified. The gene that was affected was the Neuronal Calcium Sensor protein Hippocalcin (HPCA) containing an N75K point mutation. The authors then searched a database of people suffering with dystonia and found another patient who also had a mutation in HPCA, specifically T71N.
Both mutations in the HPCA gene are located in the EF-2 calcium binding hand. Based on the positions and location of the mutation, the authors concluded that the HPCA in the dystonia patients would be rendered non-functional. The authors came to this conclusion because the EF-2 is one of the critical calcium binding EF hands.

We disagree with the authors' conclusion that these two mutations would render the proteins non-functional. Both the mutant forms of HPCA expressed in these patients would still contain 2 functional EF hands, which should still bind calcium even if the EF-2 hand was rendered inoperable. We, therefore, propose that the HPCA proteins still function, however, at a reduced capacity.

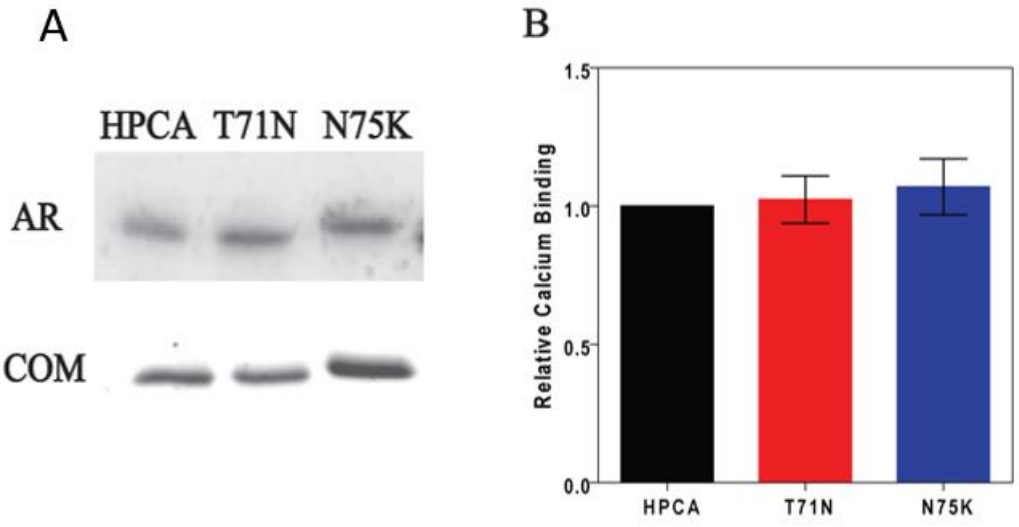

Figure 4.4.1: Direct calcium binding of the dystonia mutants.
Purified proteins were incubated with Calcium 45 as described in the materials and methods. (A) Autoradiogram (AR) of calcium bound to purified HPCA, T71N and N75K, as well as the corresponding SDS-PAGE gel stained with Coomassie (COM). (B) The mean intensity of each band from multiple experiment (N=4) was averaged and plotted relative to wild type calcium binding.

The two mutations are likely to cause minimally different effects on HPCA. Both mutations are in the EF-2 binding hand. Thr at 71 is not directly involved in calcium binding. The mutation to Asn, another polar, uncharged residue is not a great change. The Asn at 75 is directly involved in the coordination of calcium binding in the EF-2. The mutation to the positively charged Lys could potentially interfere with calcium binding, possibly knocking out the calcium binding in the EF-2 hand.

In order to test the hypothesis that the HPCA in the dystonia patients causes a dysfunctional protein, mutations of HPCA were created using site directed mutagenesis. The T71N and N75K HPCA proteins were then expressed in *E. coli* and purified as described in the Materials and Methods section.

To first demonstrate that the proteins were not simply non-functional, direct binding of calcium was performed as described in the Materials and Methods section. Briefly, purified proteins were separated on an SDS-12% poly acrylamide gel and then transferred to nitrocellulose. The blot was then incubated with calcium 45, washed, and imaged using the phosphorimager. Figure 4.4.1A, shows the result of the direct binding assay. T71N and N75K mutants do bind calcium, and they appear to bind to the same amount of calcium as the wild type (top bands labeled AR). Below the Coomassie stained loading controls (COM) are displayed. To better compare the intensities of the bands, the mean intensity for each band of multiple experiments was averaged and plotted as relative calcium binding compared to wild type HPCA (Fig 4.4.1B). The intensity of calcium binding for the HPCA mutants and the wild type are comparable over multiple experiments. This result demonstrated that the dystonia mutations, despite being in the EF-2 calcium binding hand, do bind calcium and furthermore, the binding is comparable to wild type levels. Therefore, these results demonstrate that the proteins seem unaffected in their ability to bind calcium.

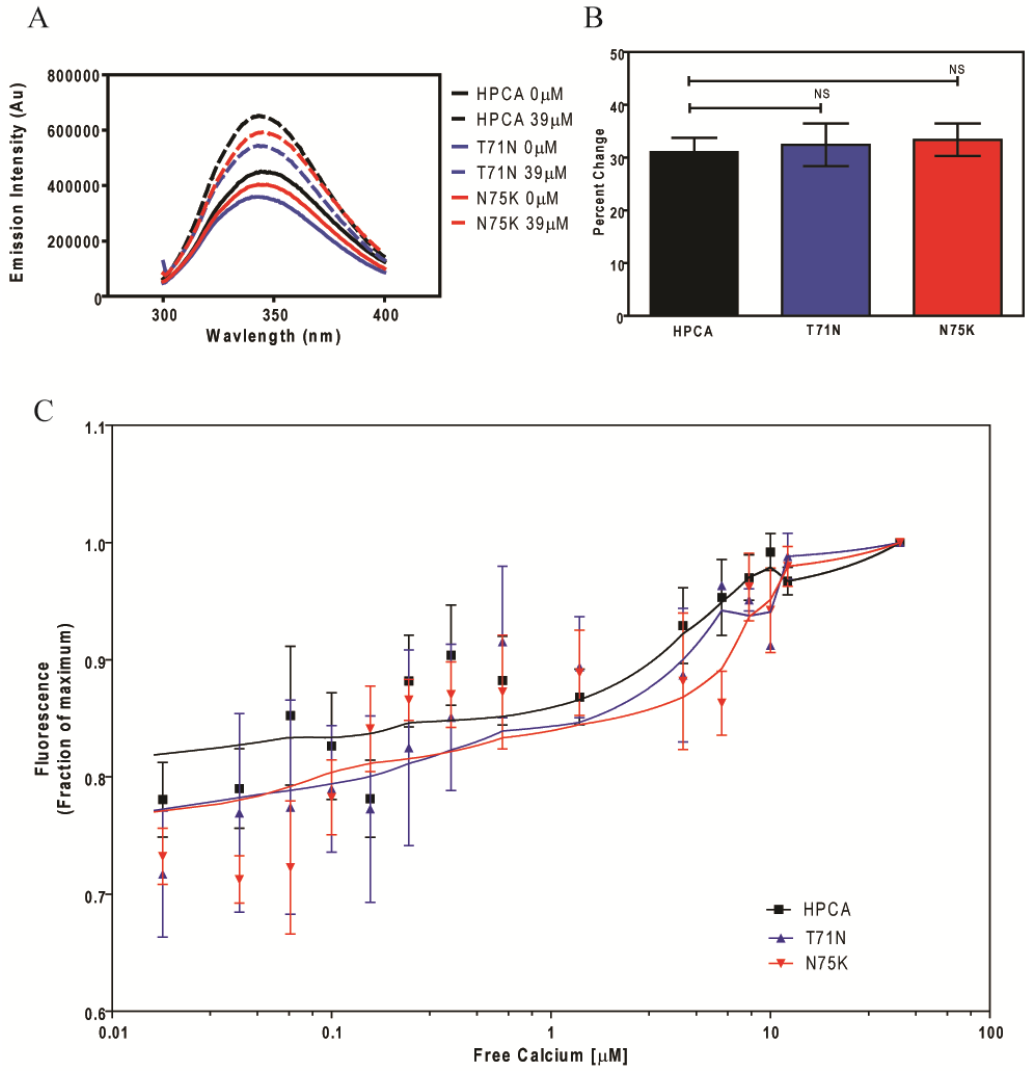

Figure 4.4.2: **Tryptophan fluorescence response of dystonia mutants to calcium binding**. (A) Represented spectra of HPCA and the dystonia mutants T71N and N75K at 0 µM and 39 µM free calcium. (B) The average (n=7) percentage increase in peak fluorescence intensities (344 nm) from 0µM, to 39µM calcium. (C) The peak fluorescence intensities at incremental free calcium concentrations were obtained and normalized to the maximum (at 39µM free calcium). Data for selected calcium concentrations are presented as mean ± SEM (n=7).

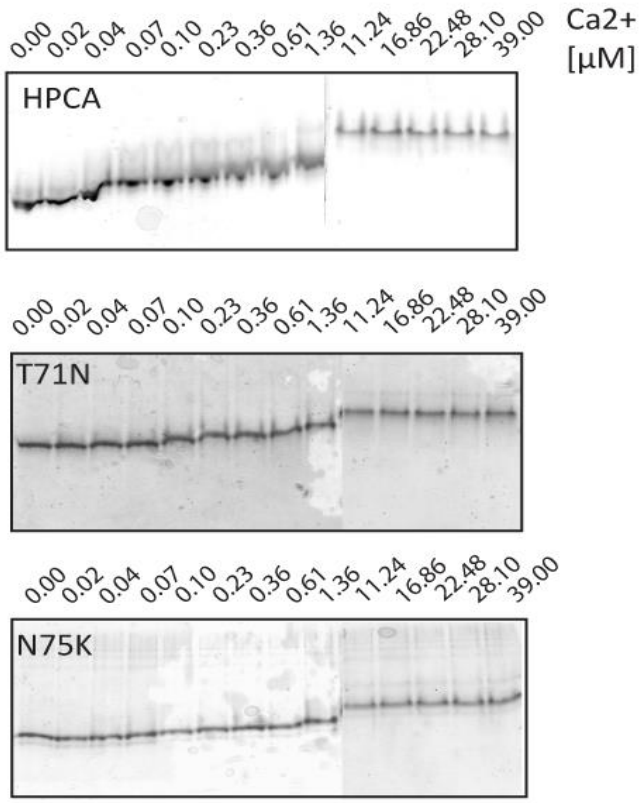

Figure 4.4.3: Effect of Dystonia mutations on calcium-induced mobility shift on native gels.

Purified HPCA, T71N and N75K were incubated with increasing free calcium concentrations and run under native conditions as described in the Materials and Methods section.

The possibility remained that the proteins could bind calcium, but not respond to the binding of calcium. To investigate this possibility, tryptophan fluorescence assays were performed. The spectra of the dystonia mutant proteins were compared to wild type HPCA (Fig. 4.4.2A). No detectable red/blue shift was observed in either of the mutants in either the presence or absence of calcium. Upon addition of calcium, the fluorescence intensity of both wild type HPCA and the two mutants increased.

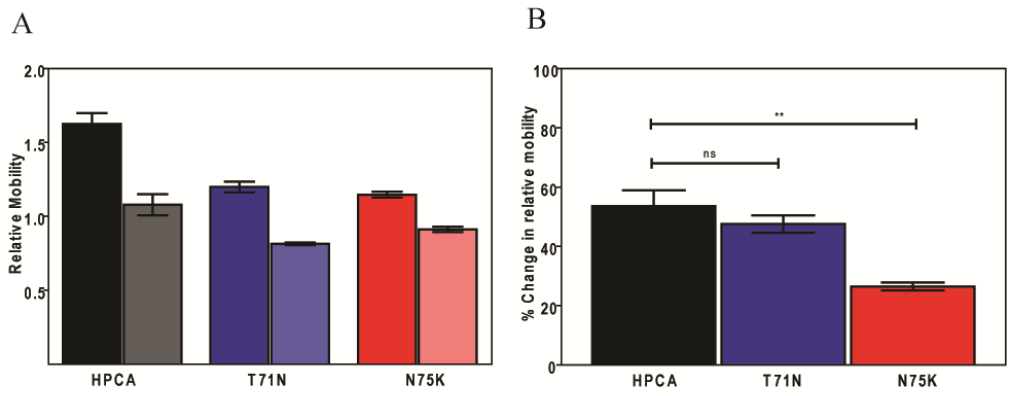

Figure 4.4.4: Effect of Dystonia mutations on calcium-induced mobility shift on native gels.

CIMSA was carried out as described in "Materials and Methods" and relative mobility values were determined. (A) The relative mobility in the presence of 0 or 39 μM of free calcium from several gels (n=6) was calculated. Data is presented as mean ± SE (B) Data is presented as mean SE for the percentage change in relative mobility. Student's t-tests were performed on pairs. T71N showed no significant difference compared to HPCA in the percentage change in relative mobility. N75K exhibited a significant difference from HPCA (*p=0.05; **p=0.02; *** p=0.001).

In order to better observe the influence of calcium on the structure, the amount of change was calculated (Fig. 4.4.2B) by averaging the percentage of change in peak fluorescence intensity from 0 μM to 39 μM free calcium for HPCA and the two mutants. T71N showed a 32% increase in fluorescence intensity upon calcium binding, while N75K demonstrated a 33% change, compared to the 31% change observed by the wild type HPCA. There was no significant difference in total percentage change between HPCA and the two mutants.

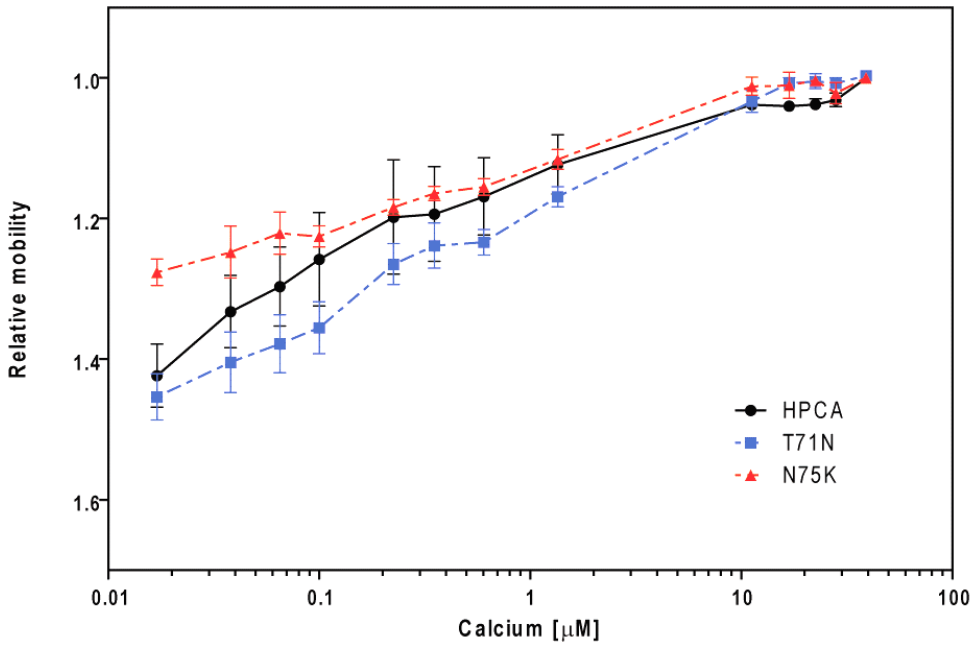

Figure 4.4.5: The response of the dystonia mutants to a range of calcium binding. The relative mobility values determined for each mutant over a range of incremental calcium concentrations were normalized to that obtained at 39 μM (maximal concentration tested).

The Dystonia mutant's calcium response over a large calcium range was then tested. The peak wavelength (344 nm) for each calcium concentration was normalized to saturating calcium at 39 μM calcium (Fig 4.4.2C). Both mutations respond to calcium in a dose dependent manner as observed in the wild type and the overall response was, very much like wild type HPCA. The tryptophan fluorescence showed that the proteins are able to both bind to, and respond to calcium and in a similar manner as the wild type protein.

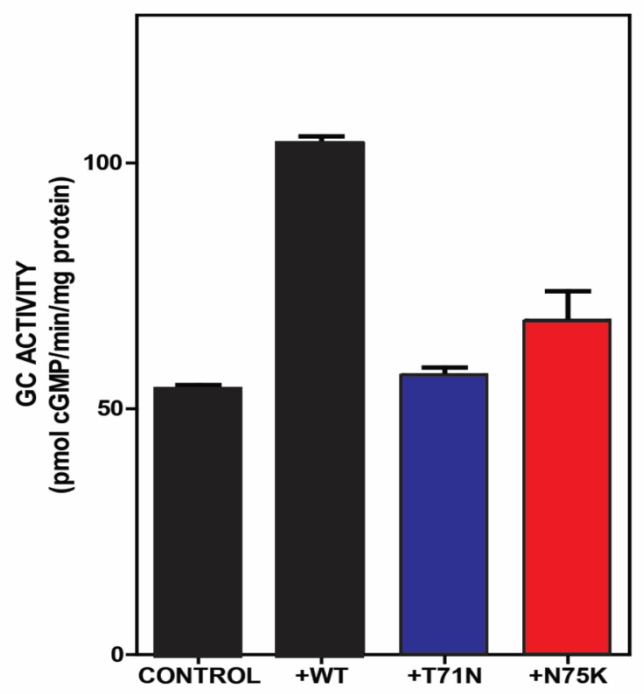

Figure 4.4.6: The ability of the Dystonia mutants to stimulate ROSGC-1.
ROS-GC1 activity was assayed as described in Materials and Methods. Stimulation by purified HPCA, T71N and N75K was measured in the presence of calcium. Results are presented as pmol cGMP/min/mg protein. Control is innate ROS-GC1 activity. Data were compiled from at least two different preparations of the proteins with two replicates each (*n*=4).

Next, the dystonia mutant's calcium response was examined by CIMSA. Multiple gels were run across the entire calcium range (Fig. 4.4.3). The band positions for 0 μM or 39 μM calcium were measured (Fig 4.4.4A). Both the T71N and the N71K HPCA proteins showed a calcium induced shift, again demonstrating that the proteins, despite their mutations, can respond to calcium. However, the initial migration position is different in both the mutants compared to HPCA, suggesting that there is a structural difference, which is reflected in a difference in surface charge compared to wild type HPCA. Next, the percentage change in the relative mobility

(Fig 4.4.4B) was calculated. Here, the N75K response is significantly different than the wild type HPCA, while the T71N mutant is HPCA-like.

Finally, the band positions of multiple gels run across the entire calcium range were normalized to that obtained at 39 μM (maximal concentration tested) (Figure 4.4.5). Overall, the T71N responds like the wild type protein over the entire range. The N75K mutation response overall is very HPCA like, however, it is less responsive to calcium at lower concentrations, CIMSA analysis demonstrated that the dystonia mutants can respond to calcium, however, there are detectible differences in the structural responses of the mutant proteins compared to HPCA.

The ability to stimulate guanylate cyclase has been demonstrated to be a critical signaling function of NCS proteins [50, 99, 109-115]. This ability was tested with the Dystonia mutants (Fig. 4.4.6). In the presence of calcium, HPCA stimulates ROSGC-1, with an increase in cGMP produced of about 50 pmol/cGMP/min/mg over basal activity. Both mutations showed a significant decrease in their ability to stimulate the membrane guanylate cyclase ROS-GC1. T71N shows no ability to stimulate ROS-GC-1. N75K shows some ability, though at a diminished rate compared to the wild type HPCA. This loss of ability to stimulate ROS-GC1 might be one of the critical functions compromised in the dystonia mutations, leading to the disease state.

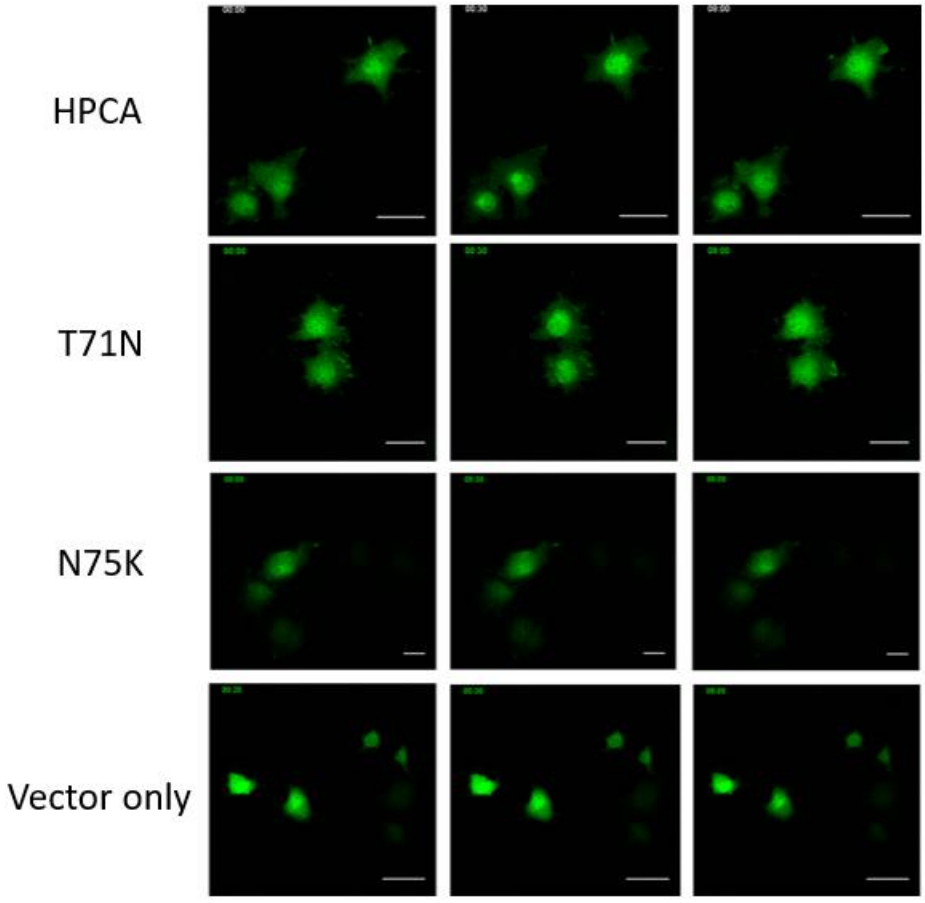

Figure 4.4.7: Calcium Induced Translocation of wild type HPCA and the dystonia mutants.

COS7 cells were transfected with wild type or mutant pCDNA3 - YFP constructs and experiments were carried out after 24 h. The cells were treated with 6 μM Histamine to increase intracellular calcium levels and live imaging was performed on a Nikon C1 laser confocal microscope equipped with a TokaiHit on-stage incubator.

HPCA has been demonstrated to cycle between the cytosol to the membrane upon the binding of calcium [100, 116]. In this manner, HPCA acts as a calcium sensor. To investigate the dystonia mutations effect on this cycling ability, GFP conjugated constructs were created. The constructs were then transformed into Cos-7

cells as described in the Materials and Methods section. Histamine was used to increase the intracellular calcium levels. In figure 4.4.7, the addition of histamine causes HPCA to translocate from the cytosol to the perinuclear region. Compared to HPCA, cells transfected with just YFP show no translocation ability. T71N shows the ability to translate in a manner similar to HPCA. However, the N75K mutation shows no ability to translocate, demonstrating a critical difference between the disease protein and the wild type, as well as a distinction between the two disease states.

Discussion

Dystonia is a disease that affects about 250,000 people in the United States [117, 118]. The recent discovery of the genetic cause of primary isolated type 2 dystonia allows for an opportunity to better understand the underlying causes of the disease. The original conclusion made by the discoverers of the HPCA mutations that resulted in dystonia was that the mutations in HPCA would render the protein inoperable. The authors made this claim because of the location of the mutations, which are in the calcium binding EF-2 hand. N75 is thought to coordinate calcium. The authors went on to conclude that a loss of HPCA causes dystonia, because HPCA knocked out neuronal astrocytes, did not function properly [104]. Our work has demonstrated that this conclusion in-fact erroneous.

First, we demonstrated that the mutant HPCA could bind calcium and that the binding was comparable to the wild type protein. While the experiment did not rule out the possibility of a lowered affinity for calcium, it did reveal that calcium could still bind to the EF-2 hand in both the N75K and T71N mutants in a comparable

manner to the wild type protein. Additional experiments tested over a range of lower free calcium concentrations would reveal this possibility.

Because the mutant proteins could effectively bind to calcium, it was important to understand how the proteins responded to calcium. Tryptophan fluorescence and CIMSA experiments were used to observe the calcium-induced response to calcium binding. Tryptophan fluorescence revealed that the proteins responded to calcium binding by inducing a structural shift, which was observed as an increase in fluorescence intensity. Both the T71N and N75K responded like wild type HPCA. CIMSA analyses revealed the T71N mutation had a wild-type like response to calcium binding, while N75K had a slightly reduced response to calcium binding. This result, along with the observation that the mutations altered the initial migrations of the protein position in the native system, reveals that there are structural differences in the proteins carrying dystonia mutations. These structural differences are observable when compared to HPCA, but the data show that the dystonia mutant proteins are still able to re-orient their structure and respond to calcium binding.

After it was established that the dystonia mutant proteins still retain the ability to bind and then respond to calcium, it was pertinent to look at one of the downstream effectors of HPCA. ROS-GC1 stimulation has been a demonstrated ability of HPCA in the regulation of intracellular calcium levels. Wild type HPCA can stimulate cGMP production nearly 2X. Both the N75K andT71N proteins failed to stimulate ROS-GC1. Since the proteins are binding to, and responding to calcium, it is possible that these sites in the EF-2 hands are involved in interactions with ROS-GC1. Here, we demonstrate the first clear problem with the mutant proteins. Since cGMP

regulates intracellular calcium levels, it seems likely that the dystonia mutations lead to calcium dysregulation inside the cells.

Finally, the translocation of the VILIP class of proteins has been demonstrated as a critical step in the calcium signaling process. HPCA translocated from the cytosol to the perinuclear region upon an increase in intracellular calcium levels (Fig 4.6-7). T71N showed translocation ability, and the translocation event was comparable to wild type HPCA. N75K demonstrated no ability to migrate under the same conditions. This is the first experiment where there was a distinction between the two dystonia mutations.

These experiments highlighted several conclusions overlooked by the original authors. First, the proteins retain the ability to bind calcium. They can bind to and respond to calcium in a manner similar to wild type HPCA, with respect to the calcium induced structural reorientation. The mutant proteins cannot stimulate ROS-GC1, showing a critical defect in their functions. Finally, we identified a difference between the two mutations, T71N and N75K, with respect to their ability to translocate. These results point to a calcium dysregulation issue rather than a knockout of a gene.

The malfunctioning dystonia proteins T71N and N75K differed in the severity of the effects of the mutations. The Charlesworth et al group went on to describe the patient's symptoms with the different dystonia mutations. People with the T71N mutation were described as having a mild form of dystonia. T71N still retains the ability to translocate upon the addition of histamine, inside of COS-7 cells, despite its inability to stimulate ROS-CG1.The N75K patients had a more severe form of the

disease. N75K was not able to stimulate ROS-CG1 and lacked the ability to translocate. This distinction is critical in understanding dystonia and how mutations correlate to physiological symptoms.

5. Discussion

The circadian clock needs to be both robust and sensitive to environment. On one hand, it is robust to overcome disturbances to maintain normal body functions; on the other hand, it is also forced to be in synchronization with the environment. For example, jet lag happens due to the circadian clock being robust; however, it diminishes because the center of body clock, the suprachiasmatic nucleus (SCN), receives light cues. Therefore, how the body clock receives and processes extrinsic factors needs to be precisely regulated. The basis for circadian phenomena are molecular oscillators which form the transcriptional and post-translational feedback loops [5]. The self-sustained system provides an approximately 24 hr cycle which is reset to exactly 24 hours by daylight [1, 2]. The current understanding of photoentrainment is that the SCN receives light signals from the eye through the RHT. Calcium is known to be involved in photoentrainment [8, 119]. Calcium regulates diverse cellular process such as vesicular trafficking, apoptosis and synapse signal transmission. Calcium signaling can be a brief localized spike or a global increase. In neurons, numerous neuronal functions are triggered by changes in free calcium concentrations. [99, 120, 121]. The transduction of calcium change requires a group of calcium sensors.

In our search for calcium sensor proteins that could contribute to photoentrainment, we were guided by our knowledge from phototransduction, the first step in vision. Light, calcium and cyclic GMP are interlocked in a negative feedback regulatory loop in phototransduction. Light causes a reduction in cyclic

GMP levels through activation of phosphodiesterase, leading to closure of cyclic nucleotide-gated calcium channels. This results in hyperpolarization. Restoration to ground state occurs by up-regulation of mGC by calcium-sensor proteins GCAP1 and GCAP2. Subsequently, the interplay between calcium and cyclic GMP through mGC and calcium-sensor proteins has been demonstrated in multiple neuronal systems [9, 10, 46]; reviewed in: [13, 15, 109, 122]]. Those studies lead us to focus on the group of proteins: NCS proteins.

The NCS proteins are responsible for calcium related signal transduction. It is crucial for a cell to sense different levels of calcium, even negative changes in calcium concentrations. NCS proteins can sense the change by binding to calcium, undergoing conformational change, move to a different location inside the cell and bind with a wide range of partners.

Through the results presented earlier, we have identified NCALD and S100B as potential regulators of photoentrainment. Despite several attempts, a knockout mouse for NCALD could not be developed, since the loss of its function is embryonically lethal. Other methods are in development to analyze the physiology. However, S100BKO mice are available and results (Fig. 5.1) suggest that S100B function is critical for robust circadian rhythms.

1. Translocation ability-NCALD, HPCA and S100B

The Neuronal Calcium Sensor (NCS) family are characterized by 4 EF-hand motifs which are helix-loop-helix structures that bind to calcium [105]. The family consists of 14 members: Frequenin (also known as NCS1), Recoverin, Kv Potassium-Channel Interacting Proteins types 1 through 4 (KChIP 1-4), Guanylate Cyclase

Activating Proteins types 1 through 3 (GCAP 1-3), Visinin-like Protein type 1 (VILIP1; gene ID VSNL1), Neurocalcin Delta (NCALD), Hippocalcin (HPCA) and hippocalcin-like proteins type 1 and 4 (HPCAL1 & HPCAL4).[98] S100 family members contain only two EF-hand helix-loop-helix calcium binding domains and they are classified as calcium binding proteins (CaBP). [123, 124]

Members of NCS proteins are amino-terminally myristoylated by N-myristoyl transferase. The myristoyl group allows for the interaction with hydrophobic fragments, which facilitates translocation from cytosol to membrane fractions [97-99]. It has been demonstrated that the translocation of HPCA in hippocampal neurons play a physiological role in Ca^{2+}-dependent local activation of specific molecular targets[100]. Taking together, N-myristoyl switch allows the proteins to respond spatially to a calcium signal. The mechanism has been demonstrated first in recoverin and then also in other NCS proteins [125-127]. In the calcium-free state, the N-terminal myristoyl group is sequestered inside. In the calcium-bound state, the protein undergoes a conformational change and the myristoyl group extrudes from the center, which allows the protein to interact with lipid bilayers [19, 120]. This structural change can be detected as electrophoretic mobility shift in denatured protein gels [128].

The S100 proteins are a group of proteins which consist of at least 25 members in human, including S100B. The proteins are dimeric, having two “EF-hand” calcium binding motifs in each subunit. Most S100 proteins can bind calcium and undergo a conformational change which allows them to control cellular activity by interacting with other proteins [reviewed in:[23]].

Our results showed that unlike most of the NCS proteins, S100B does not translocate upon calcium increase, which could be due to the fact that S100B does not contain the N-terminal myristoyl group. And this is also consistent with the result from our lab that S100B does not show mobility shift in in denatured protein gels between calcium free and calcium bound state [128].

Translocation studies using NCALD and S100B constructs in BiFC suggest that NCALD serves as a chaperon for S100B. We also demonstrate the different kinetics of translocation between NCALD and HPCA, which suggests a mechanism how a cell can sense different levels of calcium and respond differently by expressing either NCALD or HPCA, or both together. This finding also raises the intriguing possibility that other NCS proteins may also interact with S100B and each such complex may have different roles in different types of cells. Some results are provided below that assert a role for S100B in circadian clock, especially the photoentrainment aspect of it.

2. S100B KO mice exhibit altered circadian rhythms

Two different approaches were used: activity or wheel running were monitored for both wild type mice and S100B knock out mice. For activity monitoring, mice were maintained at L: D cycles over 24 hours for several days.

Further experiments were carried out through activity measurements. A chip detector was put inside each mouse. When the mouse moves, it triggers a spike, so each black dot represents the activity of the animal. After 2 months, the data were collected and analyzed. Both wild type mice (Fig. 5.1A) and S100B knock out mice (Fig. 5.1B) were kept in either LD cycles or DD cycles, as indicated.

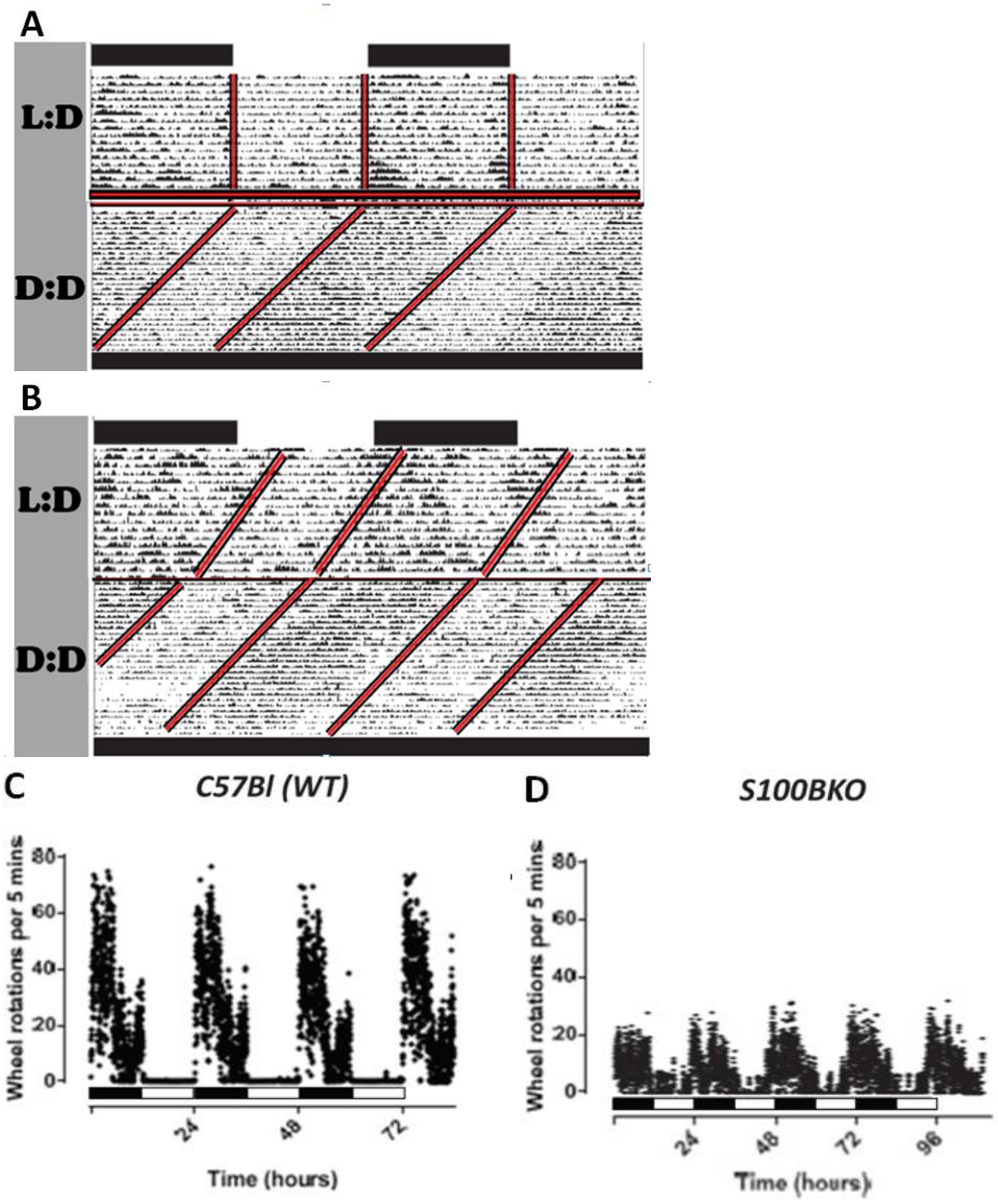

Fig.5.1 S100B KO mice lose photoentrainment?

The overall activities of both wild type mice **(A)** and S100B knock out mice **(B)** were monitored in both LD cycles and DD cycles. The wheel running activities of both wild type mice **(C)** and S100B knock out mice **(D)** were monitored in both LD cycles and DD cycles.

In LD cycles, the wild type animal exhibited 24 hours activity cycles. Because the endogenous clock period of mice is 23.5 hours, the activity pattern of wild type mice was 0.5 hour ahead each day in DD cycles (where positive slopes were drawn in DD cycles of fig 5.1A). However, the activity patterns of S100B knock out mice were 0.5 hour ahead each day in both DD cycles and LD cycles, suggesting that the animals exhibit an endogenous clock regardless of whether or not they are exposed to light. The animals, thus, were compromised in their ability to be entrained by light. Further analyses of the data are in progress.

Wheel-running activity is affected by loss of S100B function in two distinct ways: the level of activity is significantly lowered in the S100BKO mice; the rhythm is also affected when compared to the wild-type animals.

These results, together with the interaction established between NCALD and S100B, argue that the interaction may play a critical role in phase setting in circadian rhythms. An additional aspect that arose out of these findings was the differing kinetics in translocation between NCALD and HPCA. NCALD, HPCA and S100B have all been implicated in Alzheimer's disease and aging (Unpublished data from this laboratory). S100B function appears to be critical for inflammatory responses [129]. One common link among these physiological processes, including circadian rhythms, is the redox state. Therefore, it was of interest to examine if NCALD and HPCA were also sensitive to the redox state of the cell.

3. NCALD and HPCA as Redox Sensors

Generally, cells maintain a relatively reducing intracellular environment compared to the extracellular fluid. Inflammation and aging are found to increase

cytosolic redox potential. Oxidative modifications regulate protein structure and function by reactive oxygen species (ROS) such as hydrogen peroxide (H_2O_2). Cellular antioxidant systems buffer intracellular redox potential by reversible oxidation of proteins with cysteine residues [130-133].

Some of the NCS proteins have been demonstrated to be redox sensitive proteins, like recoverin and VILIP1 [134, 135]. We investigated whether NCALD and HPCA represent oxidative stress sensors in cells as well as the functions of cysteine residues in this function. In this study, we demonstrated that both NCALD and HPCA undergo reversible oxidative stress-induced structural change. This structural change could be detected in native gel mobility shift assay, which was previously used to detect the calcium-induced structural change of NCS proteins [128].

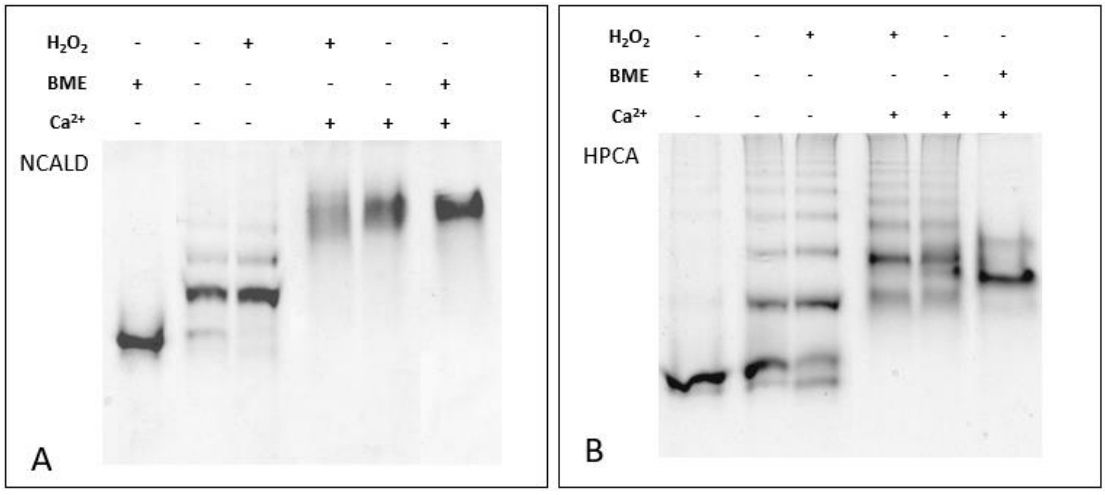

Fig. 5.2: Effect of oxidation on CIMSA:

NCALD and HPCA were subjected to CIMSA under reduced (betamercaptoethanol-added) or oxidized (H_2O_2-added) conditions. Different calcium concentrations were obtained using 0 μM to 39 μM calibration buffers.

NCALD and HPCA have two cysteine residues respectively. Cys38 is localized in the N-terminal region of the inactive EF-hand 1. Cys185 is not part of an EF-hand and is localized in the C-terminus of both proteins. Between these two, Cys38 is highly conserved through NCS family except for GCAP3. Cys185 is only conserved in NCALD, HPCA, HPCAL1, HPCAL4 and VSNL1. (Fig 5.3)

In order to investigate the roles of cysteine residues in NCALD and HPCA on redox response, we created Cys mutants on both NCALD and HPCA by site-directed mutagenesis: NCALDCys38Ala (NCC38A), NCALDCys185Ala (NCC185A), HPCACys38Ala (HCC38A), HPCACys185Ala (HCC185A), NCALDCys38AlaCys185Ala (NCC38AC185A), and HPCACys38AlaCys185Ala (HCC38AC185A).

The conformational changes detected by native gel are abolished in double cysteine mutants for both NCALD and HPCA, which suggest that the cysteine residues are critical for the function. Between the two, Cys185 is dominant over Cys38 in redox sensing function. A lower purification yield of the mutants, especially the double mutants, suggests that the cysteine residues are probably critical for the proteins to fold properly. Preliminary data from membrane binding assay suggest the cysteine residues also affect the translocation property of both NCALD and HPCA. Further experiments are underway to get a better understanding of the role of the two cysteine residues and if they affect translocation of the proteins.

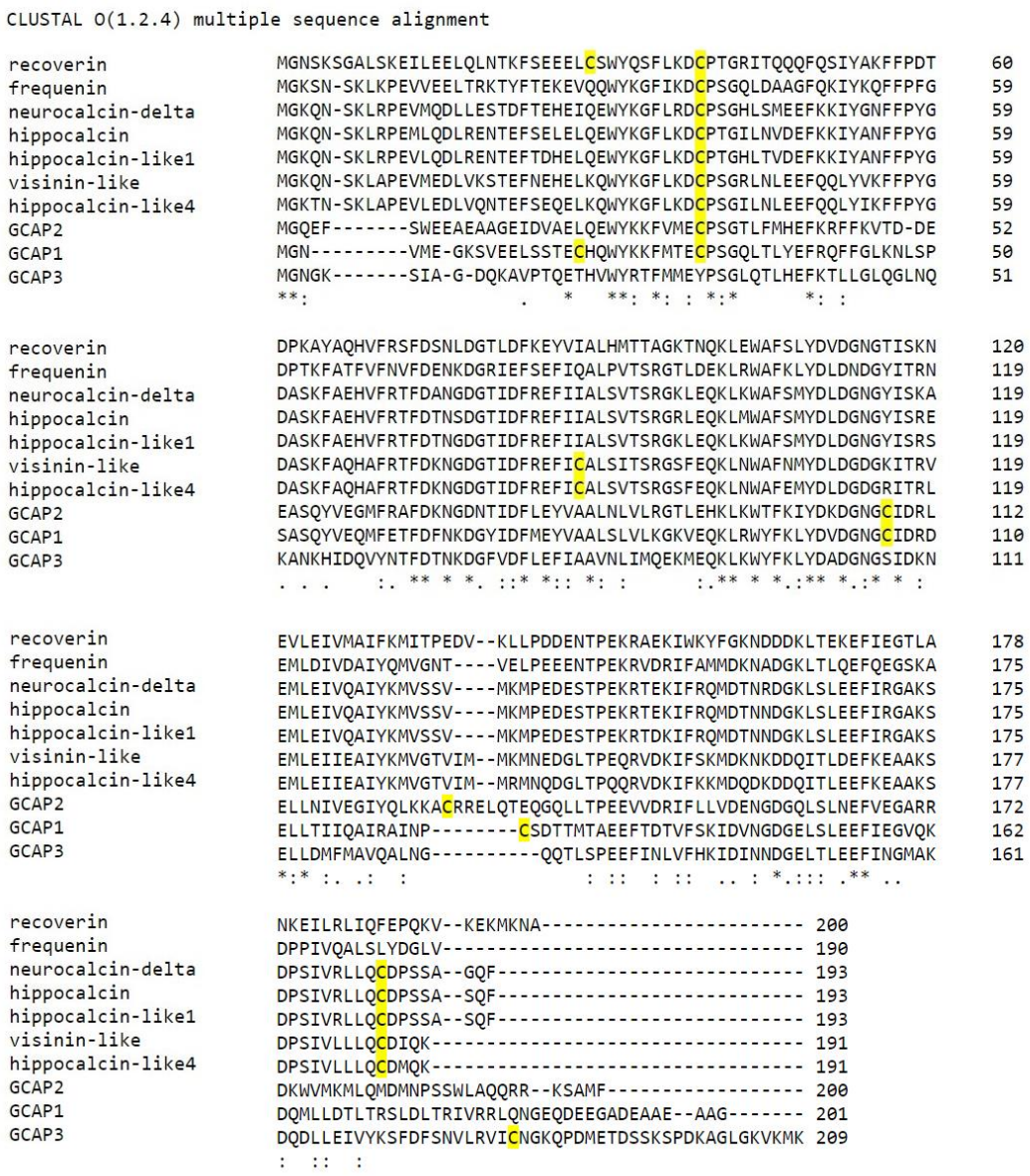

Fig. 5.3: Alignment of NCS proteins to highlight Cysteine residues.

Sequence alignment of NCS proteins using Clustal 0 (1.2.4). Cysteine residues are highlighted.

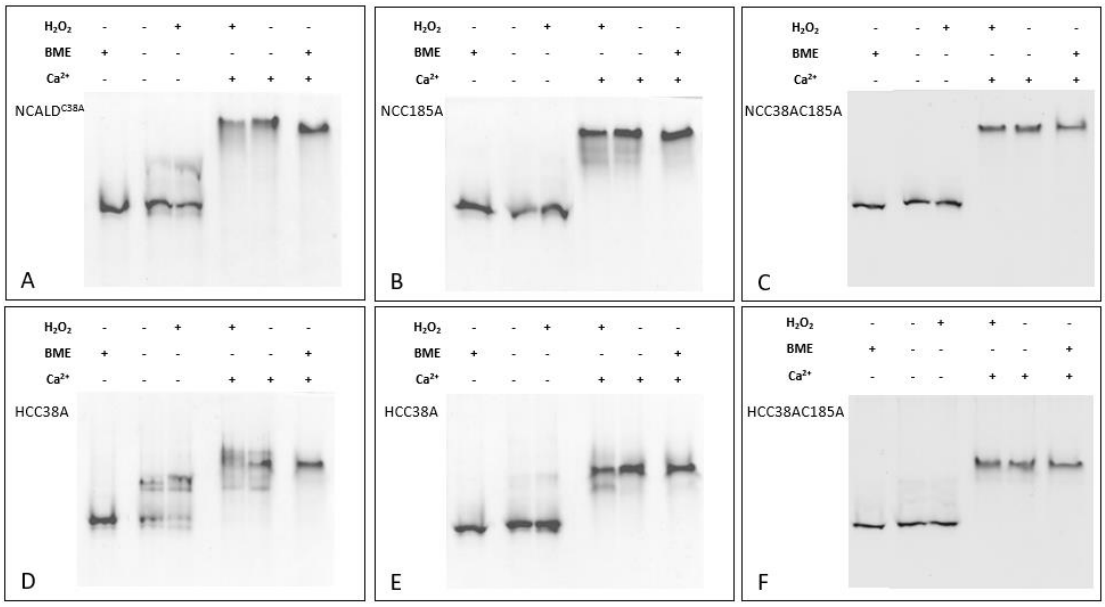

Fig. 5.4: Effect of Cys mutations on CIMSA: NCALD and HPCA – wild-type and mutants - were subjected to CIMSA under reduced (betamercaptoethanol-added) or oxidized (H_2O_2-added) conditions. Different calcium concentrations were obtained using 0 μM to 39 μM calibration buffers.

6. Summary and Conclusions

In this study, we have

1. suggested that NCALD and S100B contribute to circadian rhythms, especially photoentrainment;
2. demonstrated that NCALD binds to S100B *in vitro* in a calcium dependent manner. HPCA did not bind with S100B as well in vitro. However, both NCALD and HPCA could interact with S100B in vivo as demonstrated through the BIFC system;
3. discovered that NCS protein-S100B interactions are necessary to translocate S100B upon changes in cellular calcium;
4. identified kinetic differences in translocation between NCALD-S100B and HPCA-S100B complexes; and
5. shown that translocation is a critical aspect of signal transduction at least in HPCA; one of the mutations associated with Dystonia render the protein dysfunctional.

Understanding the molecular interaction between NCALD and HPCA proteins and S100B has provided valuable insights into their potential roles in different neuronal functions. Generation of a tissue-specific NCALD-KO will be necessary to conclusively demonstrate its role in circadian rhythm.

7. References

1. Ripperger, J.A., C. Jud, and U. Albrecht, *The daily rhythm of mice.* FEBS Lett, 2011. **585**(10): p. 1384-92.

2. Hogenesch, J.B. and E.D. Herzog, *Intracellular and intercellular processes determine robustness of the circadian clock.* FEBS Lett, 2011. **585**(10): p. 1427-34.

3. Hauw, J.J., et al., *Neuropathology of sleep disorders: a review.* Journal of neuropathology and experimental neurology, 2011. **70**(4): p. 243-52.

4. Golombek, D.A. and R.E. Rosenstein, *Physiology of circadian entrainment.* Physiological reviews, 2010. **90**(3): p. 1063-102.

5. Ko, C.H. and J.S. Takahashi, *Molecular components of the mammalian circadian clock.* Hum Mol Genet, 2006. **15 Spec No 2**: p. R271-7.

6. Whalley, K., *Circadian rhythms: Calcium sets the tempo.* Nat Rev Neurosci, 2011. **12**(8): p. 434-5.

7. Golombek, D.A., et al., *Signaling in the mammalian circadian clock: the NO/cGMP pathway.* Neurochemistry international, 2004. **45**(6): p. 929-36.

8. Golombek, D.A., et al., *From light to genes: moving the hands of the circadian clock.* Front Biosci, 2003. **8**: p. s285-93.

9. Venkataraman, V., et al., *Rod outer segment membrane guanylate cyclase type 1-linked stimulatory and inhibitory calcium signaling systems in the pineal gland: biochemical, molecular, and immunohistochemical evidence.* Biochemistry, 2000. **39**(20): p. 6042-52.

10. Duda, T., et al., *Negatively calcium-modulated membrane guanylate cyclase signaling system in the rat olfactory bulb.* Biochemistry, 2001. **40**(15): p. 4654-62.

11. Venkataraman, V., et al., *Neurocalcin delta Modulation of ROS-GC1, a New Model of Ca(2+) Signaling.* Biochemistry, 2008.

12. Baehr, W. and K. Palczewski, *Guanylate cyclase-activating proteins and retina disease.* Sub-cellular biochemistry, 2007. **45**: p. 71-91.

13. Duda, T. and K.W. Koch, *Calcium-modulated membrane guanylate cyclase in synaptic transmission?* Mol Cell Biochem, 2002. **230**(1-2): p. 107-16.

14. Stephen, R., et al., *Ca2+ -dependent regulation of phototransduction.* Photochemistry and photobiology, 2008. **84**(4): p. 903-10.

15. Venkataraman, V. and R.G. Nagele, *Calcium-sensitive ROS-GC1 signaling outside of photoreceptors: a common theme.* Mol Cell Biochem, 2002. **230**(1-2): p. 117-24.

16. Burgoyne, R.D., et al., *Neuronal Ca2+-sensor proteins: multitalented regulators of neuronal function.* Trends Neurosci, 2004. **27**(4): p. 203-9.

17. Vijay-Kumar, S. and V.D. Kumar, *Neurocalcin. Role in neuronal signaling.* Methods Mol Biol, 2002. **172**: p. 261-79.

18. Ladant, D., *Calcium and membrane binding properties of bovine neurocalcin delta expressed in Escherichia coli.* J Biol Chem, 1995. **270**(7): p. 3179-85.

19. Zozulya, S. and L. Stryer, *Calcium-myristoyl protein switch.* Proc Natl Acad Sci U S A, 1992. **89**(23): p. 11569-73.

20. Burgoyne, R.D., et al., *Differential use of myristoyl groups on neuronal calcium sensor proteins as a determinant of spatio-temporal aspects of Ca2+ signal transduction.* Journal of Biological Chemistry, 2002. **277**(16): p. 14227-14237.

21. II, R.L.S., *Neurocalcin δ: the hands that set the clock*, in *Cell Biology*. 2009, University of Medicine and Dentistry of New Jersey.

22. Krishnan, A., et al., *Structural, biochemical, and functional characterization of the calcium sensor neurocalcin delta in the inner retinal neurons and its linkage with the rod outer segment membrane guanylate cyclase transduction system.* Biochemistry, 2004. **43**(10): p. 2708-23.

23. Rezvanpour, A. and G.S. Shaw, *Unique S100 target protein interactions.* Gen Physiol Biophys, 2009. **28 Spec No Focus**: p. F39-46.

24. Okazaki, K., et al., *S100 beta is a target protein of neurocalcin delta, an abundant isoform in glial cells.* Biochem J, 1995. **306 (Pt 2)**: p. 551-5.

25. Takamatsu, K. and T. Noguchi, *Hippocalcin: a calcium-binding protein of the EF-hand superfamily dominantly expressed in the hippocampus.* Neurosci Res, 1993. **17**(4): p. 291-5.

26. Noguchi, H., et al., *Lack of hippocalcin causes impairment in Ras/extracellular signal-regulated kinase cascade via a Raf-mediated activation process.* J Neurosci Res, 2007. **85**(4): p. 837-44.

27. Kobayashi, M., et al., *Hippocalcin-deficient mice display a defect in cAMP response element-binding protein activation associated with impaired spatial and associative memory.* Neuroscience, 2005. **133**(2): p. 471-84.

28. Charlesworth, G., et al., *Mutations in HPCA Cause Autosomal-Recessive Primary Isolated Dystonia.* The American Journal of Human Genetics. **96**(4): p. 657-665.

29. Hogenesch, J.B. and H.R. Ueda, *Understanding systems-level properties: timely stories from the study of clocks.* Nat Rev Genet, 2011. **12**(6): p. 407-16.

30. McClung, C.A., *How might circadian rhythms control mood? Let me count the ways.* Biol Psychiatry, 2013. **74**(4): p. 242-9.

31. McClung, C.A., *Mind your rhythms: an important role for circadian genes in neuroprotection.* J Clin Invest, 2013. **123**(12): p. 4994-6.

32. Ramkisoensing, A. and J.H. Meijer, *Synchronization of Biological Clock Neurons by Light and Peripheral Feedback Systems Promotes Circadian Rhythms and Health.* Front Neurol, 2015. **6**: p. 128.

33. Takeda, N. and K. Maemura, *The role of clock genes and circadian rhythm in the development of cardiovascular diseases.* Cell Mol Life Sci, 2015. **72**(17): p. 3225-34.

34. Barion, A., *Circadian rhythm sleep disorders.* Disease-a-month : DM, 2011. **57**(8): p. 423-37.

35. Li, S., et al., *[The progress of studies on the relation between circadian rhythm disruption and cancer]*. Sheng Wu Yi Xue Gong Cheng Xue Za Zhi, 2012. **29**(5): p. 991-4.

36. Chan, M.C., et al., *Circadian rhythms: from basic mechanisms to the intensive care unit.* Crit Care Med, 2012. **40**(1): p. 246-53.

37. Yu, E.A. and D.R. Weaver, *Disrupting the circadian clock: gene-specific effects on aging, cancer, and other phenotypes.* Aging (Albany NY), 2011. **3**(5): p. 479-93.

38. Grote, L., et al., *Nocturnal hypertension and cardiovascular risk: consequences for diagnosis and treatment.* J Cardiovasc Pharmacol, 1994. **24 Suppl 2**: p. S26-38.

39. Pilcher, J.J., K.R. Michalowski, and R.D. Carrigan, *The prevalence of daytime napping and its relationship to nighttime sleep.* Behav Med, 2001. **27**(2): p. 71-6.

40. Yang, G., et al., *Knitting up the raveled sleave of care.* Sci Transl Med, 2013. **5**(212): p. 212rv3.

41. Partch, C.L., C.B. Green, and J.S. Takahashi, *Molecular architecture of the mammalian circadian clock.* Trends Cell Biol, 2014. **24**(2): p. 90-9.

42. Miranda, M., *The Role of EFhand1 in Calcium-dependent Activation of Neuroccalcin delta and Hippocalcin*, in *Cell Biology*. 2010, UMDNJ: Sratford, NJ. p. 38.

43. Patel, S.K., *The role of EF1 Hand in Calcium-dependent Activation of Neurocalcin delta*, in *Cell Biology*. 2008, UMDNJ: Stratford, NJ. p. 48.

44. Smale, S.T., *Calcium Phosphate Transfection of 3T3 Fibroblasts.* Cold Spring Harbor Protocols, 2010. **2010**(2): p. pdb.prot5372.

45. Venkataraman, V., et al., *Calcium-modulated guanylate cyclase transduction machinery in the photoreceptor--bipolar synaptic region.* Biochemistry, 2003. **42**(19): p. 5640-8.

46. Venkataraman, V., et al., *Neurocalcin delta modulation of ROS-GC1, a new model of Ca(2+) signaling.* Biochemistry, 2008. **47**(25): p. 6590-601.

47. Venkataraman, V., T. Duda, and R.K. Sharma, *The alpha(2D/A)-adrenergic receptor-linked membrane guanylate cyclase: a new signal transduction system in the pineal gland.* FEBS Lett, 1998. **427**(1): p. 69-73.

48. Schindelin, J., et al., *Fiji: an open-source platform for biological-image analysis.* Nat Methods, 2012. **9**(7): p. 676-82.

49. Krishnan, A., et al., *Single-column purification of the tag-free, recombinant form of the neuronal calcium sensor protein, hippocalcin expressed in Escherichia coli.* Protein Expr Purif, 2016. **123**: p. 35-41.

50. Krishnan, A., et al., *Hippocalcin, new Ca(2+) sensor of a ROS-GC subfamily member, ONE-GC, membrane guanylate cyclase transduction system.* Mol Cell Biochem, 2009. **325**(1-2): p. 1-14.

51. Hurst, W.J., D. Earnest, and M.U. Gillette, *Immortalized suprachiasmatic nucleus cells express components of multiple circadian regulatory pathways.* Biochem Biophys Res Commun, 2002. **292**(1): p. 20-30.

52. Duda, T., et al., *A novel calcium-regulated membrane guanylate cyclase transduction system in the olfactory neuroepithelium.* Biochemistry, 2001. **40**(40): p. 12067-77.

53. Brunelle, J.L. and R. Green, *One-dimensional SDS-polyacrylamide gel electrophoresis (1D SDS-PAGE).* Methods Enzymol, 2014. **541**: p. 151-9.

54. Laemmli, U.K., *Cleavage of structural proteins during the assembly of the head of bacteriophage T4.* Nature, 1970. **227**(5259): p. 680-5.

55. Moore, R.Y. and V.B. Eichler, *Loss of a circadian adrenal corticosterone rhythm following suprachiasmatic lesions in the rat.* Brain Res, 1972. **42**(1): p. 201-6.

56. Stephan, F.K. and I. Zucker, *Circadian rhythms in drinking behavior and locomotor activity of rats are eliminated by hypothalamic lesions.* Proc Natl Acad Sci U S A, 1972. **69**(6): p. 1583-6.

57. Weaver, D.R., *The suprachiasmatic nucleus: a 25-year retrospective.* J Biol Rhythms, 1998. **13**(2): p. 100-12.

58. Harrisingh, M.C. and M.N. Nitabach, *Circadian rhythms. Integrating circadian timekeeping with cellular physiology.* Science, 2008. **320**(5878): p. 879-80.

59. Kriegsfeld, L.J., et al., *Targeted mutation of the calbindin D28K gene disrupts circadian rhythmicity and entrainment.* Eur J Neurosci, 2008. **27**(11): p. 2907-21.

60. Harrisingh, M.C., et al., *Intracellular Ca2+ regulates free-running circadian clock oscillation in vivo.* J Neurosci, 2007. **27**(46): p. 12489-99.

61. Colwell, C.S., *Circadian modulation of calcium levels in cells in the suprachiasmatic nucleus.* Eur J Neurosci, 2000. **12**(2): p. 571-6.

62. Dodd, A.N., et al., *The Arabidopsis circadian clock incorporates a cADPR-based feedback loop.* Science, 2007. **318**(5857): p. 1789-92.

63. Ding, J.M., et al., *A neuronal ryanodine receptor mediates light-induced phase delays of the circadian clock.* Nature, 1998. **394**(6691): p. 381-4.

64. Zatz, M. and J.R. Heath, 3rd, *Calcium and photoentrainment in chick pineal cells revisited: effects of caffeine, thapsigargin, EGTA, and light on the melatonin rhythm.* J Neurochem, 1995. **65**(3): p. 1332-41.

65. Ferreyra, G.A. and D.A. Golombek, *Rhythmicity of the cGMP-related signal transduction pathway in the mammalian circadian system.* Am J Physiol Regul Integr Comp Physiol, 2001. **280**(5): p. R1348-55.

66. Weber, E.T. and M. Gillette, *Endogenous circadian changes in cGMP levels in the rat suprachiasmatic nucleus.* Society ofNeuroscience Abstracts, 1990. **16**: p. 317-318.

67. Prosser, R.A., A.J. McArthur, and M.U. Gillette, *cGMP induces phase shifts of a mammalian circadian pacemaker at night, in antiphase to cAMP effects.* Proc Natl Acad Sci U S A, 1989. **86**(17): p. 6812-5.

68. Liu, C., et al., *Coupling of muscarinic cholinergic receptors and cGMP in nocturnal regulation of the suprachiasmatic circadian clock.* J Neurosci, 1997. **17**(2): p. 659-66.

69. Golombek, D.A., et al., *Signaling in the mammalian circadian clock: the NO/cGMP pathway.* Neurochem Int, 2004. **45**(6): p. 929-36.

70. Kriegsfeld, L.J., et al., *Circadian locomotor analysis of male mice lacking the gene for neuronal nitric oxide synthase (nNOS-/-).* J Biol Rhythms, 1999. **14**(1): p. 20-7.

71. Kriegsfeld, L.J., D.L. Drazen, and R.J. Nelson, *Circadian organization in male mice lacking the gene for endothelial nitric oxide synthase (eNOS-/-).* J Biol Rhythms, 2001. **16**(2): p. 142-8.

72. Sharma, R.K., *Evolution of the membrane guanylate cyclase system.* Molecular and Cellular Biochemistry, 2002. **230**: p. 3-30.

73. Chinkers, M., et al., *A membrane form of guanylate cyclase is an atrial natriuretic peptide receptor.* Nature, 1989. **338**(6210): p. 78-83.

74. Paul, A.K., et al., *Coexistence of guanylate cyclase and atrial natriuretic factor receptor in a 180-kD protein.* Science, 1987. **235**(4793): p. 1224-6.

75. Koller, K.J., et al., *Selective activation of the B natriuretic peptide receptor by C-type natriuretic peptide (CNP).* Science, 1991. **252**(5002): p. 120-3.

76. Currie, M.G., et al., *Guanylin: an endogenous activator of intestinal guanylate cyclase.* Proc Natl Acad Sci U S A, 1992. **89**(3): p. 947-51.

77. Schulz, S., et al., *Guanylyl cyclase is a heat-stable enterotoxin receptor.* Cell, 1990. **63**(5): p. 941-8.

78. Schulz, S., *C-type natriuretic peptide and guanylyl cyclase B receptor.* Peptides, 2005. **26**(6): p. 1024-34.

79. Tremblay, J., et al., *Biochemistry and physiology of the natriuretic peptide receptor guanylyl cyclases.* Mol Cell Biochem, 2002. **230**(1-2): p. 31-47.

80. Koch, K.W., T. Duda, and R.K. Sharma, *Photoreceptor Specific Guanylate Cyclases in Vertebrate Phototransduction.*, in *Guanlate Cyclase,* R.K. Sharma, Editor. 2002, Kluwer Academic Publishers: Norwell, MA, USA. p. 97-106.

81. Sharma, R.K., et al., *Calcium-modulated membrane guanylate cyclase, ROS-GC transduction machinery in sensory neurons: a universal concept.* Current Topics in Biochemical Research, 2004. **6**: p. 111-144.

82. Duda, T., et al., *Ca(2+) sensor S100beta-modulated sites of membrane guanylate cyclase in the photoreceptor-bipolar synapse.* EMBO J, 2002. **21**(11): p. 2547-56.

83. Margulis, A., et al., *Structural and biochemical identity of retinal rod outer segment membrane guanylate cyclase.* Biochem Biophys Res Commun, 1993. **194**(2): p. 855-61.

84. Shyjan, A.W., et al., *Molecular cloning of a retina-specific membrane guanylyl cyclase.* Neuron, 1992. **9**(4): p. 727-37.

85. Yang, R.B., et al., *Two membrane forms of guanylyl cyclase found in the eye.* Proc Natl Acad Sci U S A, 1995. **92**(2): p. 602-6.

86. Duda, T., R. Krishnan, and R.K. Sharma, *GCAP1, antithetical calcium sensor of ROS-GC transduction machinery.* Calcium Binding Proteins, 2006. **1**: p. 102-107.

87. Allen, G., et al., *Oscillating on borrowed time: diffusible signals from immortalized suprachiasmatic nucleus cells regulate circadian rhythmicity in cultured fibroblasts.* J Neurosci, 2001. **21**(20): p. 7937-43.

88. Earnest, D.J., et al., *Establishment and characterization of adenoviral E1A immortalized cell lines derived from the rat suprachiasmatic nucleus.* J Neurobiol, 1999. **39**(1): p. 1-13.

89. Earnest, D.J., et al., *Immortal time: circadian clock properties of rat suprachiasmatic cell lines.* Science, 1999. **283**(5402): p. 693-5.

90. Hurst, W.J., J.W. Mitchell, and M.U. Gillette, *Synchronization and phase-resetting by glutamate of an immortalized SCN cell line.* Biochem Biophys Res Commun, 2002. **298**(1): p. 133-43.

91. Gonzalez-Menendez, I., et al., *Daily rhythm of melanopsin-expressing cells in the mouse retina.* Front Cell Neurosci, 2009. **3**: p. 3.

92. Ruan, G.X., et al., *An autonomous circadian clock in the inner mouse retina regulated by dopamine and GABA.* PLoS Biol, 2008. **6**(10): p. e249.

93. Geyfman, M. and B. Andersen, *How the skin can tell time.* J Invest Dermatol, 2009. **129**(5): p. 1063-6.

94. Tanioka, M., et al., *Molecular clocks in mouse skin.* J Invest Dermatol, 2009. **129**(5): p. 1225-31.

95. O'Callaghan, D.W., et al., *Differential use of myristoyl groups on neuronal calcium sensor proteins as a determinant of spatio-temporal aspects of Ca2+ signal transduction.* J Biol Chem, 2002. **277**(16): p. 14227-37.

96. Kodama, Y. and C.D. Hu, *Bimolecular fluorescence complementation (BiFC): a 5-year update and future perspectives.* Biotechniques, 2012. **53**(5): p. 285-98.

97. Burgoyne, R.D. and J.L. Weiss, *The neuronal calcium sensor family of Ca2+-binding proteins.* Biochem J, 2001. **353**(Pt 1): p. 1-12.

98. Viviano, J., Wu, H., Venkataraman, V., *Evolutionary Interrelationships and Insights into Molecular Mechanisms of Functional Divergence: An Analysis of Neuronal Calcium Sensor Proteins.* Phylogenetics & Evolutionary Biology, 2013. **1**(4): p. 117.

99. Burgoyne, R.D., *Neuronal calcium sensor proteins: generating diversity in neuronal Ca2+ signalling.* Nat Rev Neurosci, 2007. **8**(3): p. 182-93.

100. Markova, O., et al., *Hippocalcin signaling via site-specific translocation in hippocampal neurons.* Neurosci Lett, 2008. **442**(2): p. 152-7.

101. O'Callaghan, D.W. and R.D. Burgoyne, *Role of myristoylation in the intracellular targeting of neuronal calcium sensor (NCS) proteins.* Biochem Soc Trans, 2003. **31**(Pt 5): p. 963-5.

102. O'Callaghan, D.W. and R.D. Burgoyne, *Identification of residues that determine the absence of a Ca(2+)/myristoyl switch in neuronal calcium sensor-1.* J Biol Chem, 2004. **279**(14): p. 14347-54.

103. O'Callaghan, D.W., A.V. Tepikin, and R.D. Burgoyne, *Dynamics and calcium sensitivity of the Ca2+/myristoyl switch protein hippocalcin in living cells.* J Cell Biol, 2003. **163**(4): p. 715-21.

104. Charlesworth, G., et al., *Mutations in HPCA cause autosomal-recessive primary isolated dystonia.* Am J Hum Genet, 2015. **96**(4): p. 657-65.

105. Kumar, V.D., et al., *Crystallization and preliminary X-ray crystallographic studies of recombinant bovine neurocalcin delta.* Proteins, 1996. **25**(2): p. 261-4.

106. O'Callaghan, D.W., et al., *Residues within the myristoylation motif determine intracellular targeting of the neuronal Ca2+ sensor protein KChIP1 to post-ER transport vesicles and traffic of Kv4 K+ channels.* J Cell Sci, 2003. **116**(Pt 23): p. 4833-45.

107. Kim, K.S., et al., *Hippocalcin and KCNQ channels contribute to the kinetics of the slow afterhyperpolarization.* Biophys J, 2012. **103**(12): p. 2446-54.

108. Moon, C., et al., *Calcium-sensitive particulate guanylyl cyclase as a modulator of cAMP in olfactory receptor neurons.* J Neurosci, 1998. **18**(9): p. 3195-205.

109. Baehr, W. and K. Palczewski, *Guanylate cyclase-activating proteins and retina disease.* Subcell Biochem, 2007. **45**: p. 71-91.

110. Howes, K.A., et al., *GCAP1 rescues rod photoreceptor response in GCAP1/GCAP2 knockout mice.* EMBO J, 2002. **21**(7): p. 1545-54.

111. Hwang, J.Y., et al., *Regulatory modes of rod outer segment membrane guanylate cyclase differ in catalytic efficiency and Ca(2+)-sensitivity.* Eur J Biochem, 2003. **270**(18): p. 3814-21.

112. Lange, C., et al., *Regions in vertebrate photoreceptor guanylyl cyclase ROS-GC1 involved in Ca(2+)-dependent regulation by guanylyl cyclase-activating protein GCAP-1.* FEBS Lett, 1999. **460**(1): p. 27-31.

113. Pettelkau, J., et al., *Structural Insights into retinal guanylylcyclase-GCAP-2 interaction determined by cross-linking and mass spectrometry.* Biochemistry, 2012. **51**(24): p. 4932-49.

114. Sakurai, K., J. Chen, and V.J. Kefalov, *Role of guanylyl cyclase modulation in mouse cone phototransduction.* J Neurosci, 2011. **31**(22): p. 7991-8000.

115. Stephen, R., K. Palczewski, and M.C. Sousa, *The crystal structure of GCAP3 suggests molecular mechanism of GCAP-linked cone dystrophies.* J Mol Biol, 2006. **359**(2): p. 266-75.

116. Dovgan, A.V., et al., *Decoding glutamate receptor activation by the Ca2+ sensor protein hippocalcin in rat hippocampal neurons.* Eur J Neurosci, 2010. **32**(3): p. 347-58.

117. Balint, B. and K.P. Bhatia, *Dystonia: an update on phenomenology, classification, pathogenesis and treatment.* Curr Opin Neurol, 2014. **27**(4): p. 468-76.

118. Surgeons, A.A.o.N. *Dystonia*. 2016; Available from: http://www.aans.org/patient%20information/conditions%20and%20treatments/dystonia.aspx.

119. Golombek, D.A. and R.E. Rosenstein, *Physiology of circadian entrainment.* Physiol Rev, 2010. **90**(3): p. 1063-102.

120. Burgoyne, R.D. and L.P. Haynes, *Understanding the physiological roles of the neuronal calcium sensor proteins.* Mol Brain, 2012. **5**(1): p. 2.

121. Zamponi, G.W. and K.P. Currie, *Regulation of Ca(V)2 calcium channels by G protein coupled receptors.* Biochim Biophys Acta, 2012.

122. Stephen, R., et al., *Ca2+ -dependent regulation of phototransduction.* Photochem Photobiol, 2008. **84**(4): p. 903-10.

123. Marenholz, I., C.W. Heizmann, and G. Fritz, *S100 proteins in mouse and man: from evolution to function and pathology (including an update of the nomenclature).* Biochem Biophys Res Commun, 2004. **322**(4): p. 1111-22.

124. Zimmer, D.B., et al., *Evolution of the S100 family of calcium sensor proteins.* Cell Calcium, 2013. **53**(3): p. 170-9.

125. Bourne, Y., et al., *Immunocytochemical localization and crystal structure of human frequenin (neuronal calcium sensor 1).* J Biol Chem, 2001. **276**(15): p. 11949-55.

126. Zhou, W., et al., *Structural insights into the functional interaction of KChIP1 with Shal-type K(+) channels.* Neuron, 2004. **41**(4): p. 573-86.

127. Lemire, S., A. Jeromin, and E. Boisselier, *Membrane binding of Neuronal Calcium Sensor-1 (NCS1).* Colloids Surf B Biointerfaces, 2016. **139**: p. 138-47.

128. Viviano, J., et al., *Electrophoretic mobility shift in native gels indicates calcium-dependent structural changes of neuronal calcium sensor proteins.* Anal Biochem, 2016. **494**: p. 93-100.

129. Wu, H., et al., *Age-dependent increase of blood-brain barrier permeability and neuron-binding autoantibodies in S100B knockout mice.* Brain Res, 2016. **1637**: p. 154-67.

130. Ratnayake, S., et al., *Stabilising cysteinyl thiol oxidation and nitrosation for proteomic analysis.* J Proteomics, 2013. **92**: p. 160-70.

131. Pace, N.J. and E. Weerapana, *Diverse functional roles of reactive cysteines.* ACS Chem Biol, 2013. **8**(2): p. 283-96.

132. Hancock, J.T., R. Desikan, and S.J. Neill, *Cytochrome c, glutathione, and the possible role of redox potentials in apoptosis.* Ann N Y Acad Sci, 2003. **1010**: p. 446-8.

133. Samiec, P.S., et al., *Glutathione in human plasma: decline in association with aging, age-related macular degeneration, and diabetes.* Free Radic Biol Med, 1998. **24**(5): p. 699-704.

134. Permyakov, S.E., et al., *Recoverin as a redox-sensitive protein.* J Proteome Res, 2007. **6**(5): p. 1855-63.

135. Liebl, M.P., et al., *Dimerization of visinin-like protein 1 is regulated by oxidative stress and calcium and is a pathological hallmark of amyotrophic lateral sclerosis.* Free Radic Biol Med, 2014. **72**: p. 41-54.

8. Appendix, Abbreviations list

CaBP-calcium binding protein
cAMP - adenylyl cyclase monophosphate
cGMP- 3',5'-cyclic guanosine monophosphate
GCAP-1-Guanylyl-Cyclase Activating Protein 1
GCAP-2- Guanylyl-Cyclase Activating Protein 2
GCAP-3- Guanylyl-Cyclase Activating Protein 3
GCAPs- Guanylyl-Cyclase Activating Proteins
GC- Guanylate Cyclase
GM – Growth Medium
HPCA- Hippocalcin
mGC – membrane Guanylate Cyclase
Myr- Myristoyl
NCALD-Neurocalcin Delta
NCS- Neuronal Calcium Sensor
NCS-1 (Frequenin)- Neuronal calcium sensor 1
NM – Neuronal Medium
NO – Nitric Oxide
RHT – Retino-Hypothalamic Tract
ROS - Reactive Oxygen Species
ROSGC- Rod outer segment Guanylate cyclase
SCN – Suprachiasmatic Nucleus
VILIPs- Visinin-Like Proteins

9. Attributes

Figure 1.1- Jingyi Zhang
Figure 1.2- Jingyi Zhang, Venkat Venkataraman
Figure 4.1.1 – Venkat Venkataraman
Figure 4.1.2 – Randel Swanson, Venkat Venkataraman
Figure 4.1.3 – Randel Swanson, Venkat Venkataraman
Figure 4.1.4 – Jingyi Zhang, Randel Swanson, Venkat Venkataraman
Figure 4.1.5 – Jingyi Zhang, Randel Swanson, Venkat Venkataraman
Figure 4.1.6 – Jingyi Zhang, Teresa Duda, Venkat Venkataraman
Figure 4.1.7 – Jingyi Zhang, Randel Swanson, Venkat Venkataraman
Figure 4.1.8 – Jingyi Zhang, Randel Swanson, Venkat Venkataraman
Figure 4.1.9 – Jingyi Zhang, Randel Swanson, Venkat Venkataraman
Figure 4.2.1- Jingyi Zhang
Figure 4.2.2- Jingyi Zhang, Anu Krishnan , Venkat Venkataraman
Figure 4.2.3- Jingyi Zhang, Venkat Venkataraman
Figure 4.2.4- Jingyi Zhang
Figure 4.3.1- Jingyi Zhang
Figure 4.3.2- Jingyi Zhang
Figure 4.3.3- Jingyi Zhang, Hao Wu
Figure 4.3.4- Robert Steer, Venkat Venkataraman, Jingyi Zhang
Figure 4.4.1- Jeffrey Viviano, Anu Krishnan
Figure 4.4.2- Jeffrey Viviano
Figure 4.4.3- Jingyi Zhang, Jeffrey Viviano
Figure 4.4.4- Jingyi Zhang, Jeffrey Viviano
Figure 4.4.5- Jeffrey Viviano, Anu Krishnan
Figure 4.4.6- Anu Krishnan
Figure 4.4.7- Jingyi Zhang
Figure 5.1- Jingyi Zhang, Steve Moffett, Bradford Fischer
Figure 5.2- Jingyi Zhang
Figure 5.3- Jingyi Zhang
Figure 5.4- Jingyi Zhang, Pooja Amin